A Basis for Magnet Improvements in the U.S. Fusion Magnet Program

Joel H. Schultz, Joseph V. Minervini, Richard J. Thome
April 21, 1999
M.I.T. Plasma Science and Fusion Center Report PSFC/RR-99-6

The following is a strategic vision for magnet development, focused on the goal of improving the cost and size of superconducting and normal magnets for the magnet and inertial fusion programs. This program vision is an attempt to be responsive to the request that a development program must be able to define quantitatively the improvements in benefits and cost/benefits to our specific subsystem. At this preliminary stage, the vision statement has not yet been matched to budget, schedule, or available resources. Neither has it been correlated to a separate vision and program of improvements in analysis techniques. However, in its defense, it is - to the best of our knowledge - the first time that anyone worldwide, in either the fusion or HEP programs, has attempted to lay out a complete statement of how to improve magnet systems with quantitative goals. Due to the absence of previous visions, this must be considered preliminary, but will henceforth be a "living" document to be continually refined and expanded.

I. Overview

The United States should be developing magnet technologies that are specifically focused on the needs of the magnetic and inertial fusion programs that will substantially lower the cost of fusion power. There are primarily two ways in which a magnet technology can lower the cost of fusion: 1) by lowering the cost of the magnets themselves and 2) by reducing the size of the magnet systems, so that the cost of other fusion reactor subsystems may be reduced. That said, the normalized goodness parameter for a magnet system isn't totally clear. For instance, one could also argue that the primary virtue of a magnet is to produce a high magnetic field, since fusion power is proportional to B^4. Another virtue of a good magnet system design is the ability to absorb high nuclear flux and fluence in order to reduce the size of the neutron shield protecting the magnet system and consequently the machine as a whole. Nevertheless, in order to create a manageable and affordable program, one has to choose the goodness parameters that are the most likely to make a difference and these are:

1) The volume-specific stored energy (J/m³)
$$a = \frac{W_m}{V}$$

2) The cost-specific stored energy (J/$)
$$g = \frac{W_m}{\$}$$

3) The entropy-specific refrigeration load
$$d = \frac{P_{ref}}{P_e}$$

We maintain that maximizing α and γ, i.e. minimizing the specific cost and volume, should simultaneously develop the technologies needed for high-field. Maximizing δ is done by minimizing the wall power needed to remove a given refrigeration load. The most exciting method of maximizing δ is through the use of high-temperature superconductors.

The clearest way of ensuring that a magnet technology will simultaneously improve $\alpha, \gamma,$ and δ is to identify the goodness factors for each of the magnet components individually. In this "0-rev" vision, we propose major improvements that can be made in the following components:

(A) Superconductor
(B) Stabilizer
(C) Structure
(Ca) Conductor/Structure
(D) Insulation
(E) Thermal Isolation
(F) Joints

(G) Leads
(H) Quench Detection and Instrumentation
(I) Isolators and Feedthroughs

Two more highly important components are not considered, but are left as placemarks for a future revision:

(J) Field Errors and Tolerances
(K) Refrigeration

If important quantitative and achievable goals can be realized for all of these components individually, it should be possible to reduce the cost of fusion itself.

     As discussed above, for most fusion applications, specific volume α is more important than specific mass, since the majority of applications are constrained more by space than by the floor bearing strength. However, magnet mass is frequently tabulated in the published literature, volume almost never. Another difficulty in pinning down specific mass or volume is that it is sometimes unclear whether tables include cold mass only, gravity supports, and/or the cryostat. With those caveats, we have attempted to tabulate the mass of efficiencies of several superconducting and normal magnet systems in Table I-1:

I-1 Mass Efficiencies of Superconducting and Normal Magnets

Magnet	Stored Energy	Mass	Mass/Energy
	(MJ)	(tonnes)	(kg/kJ)
Ignitor TF	1309	96 (magnet)	0.073
		436.8 (magnet+clamps)	0.334
TFTR, TF	1366	580	0.425
PLT, TF	251	98	0.78
PDX, TF	182	73	0.401
ATC, TF	16.7	26	1.56
Alcator A, TF	24	5.8	0.335
Alcator C, TF	95	17.7	0.372
Ormak, TF	4.5	10	2.2
ISX-A, TF	19.4	12.0	0.618
ISX-B, TF	13.5	12.0	0.889
JET, TF	940	380	0.404
Zephyr, TF	1200	300	0.25
LCP	650	290	0.446
MFTF	409	341	0.834
Tore Supra	640	206	0.322
NMR Solenoid	0.4	0.082	0.205
CS Model Coil	650	150	0.231
FED	16300	4040	0.248
STARFIRE	50000	6000	0.12
WITAMIR	60,300	8,358	0.139
NUWMAK	35,700	1,540	0.043
UWMAK III	117,000	6,564	0.056
UWMAK II	233,000	25,508	0.109
UWMAK I	216,000	23,800	0.11

It is very striking how much less efficient the actual magnet systems are than the imaginary ones. The masses of paper study magnets may have to be completely discounted. However, there is a clear trend that paper studies of visionary systems to be built in the distant future weigh the least, while the masses increase from conceptual to preliminary to final design. Therefore, we might hope that, for example, the

ITER EDA or IGNITOR designs might be relatively accurate. We are not sure what the world's record is for a real magnet. Many magnet systems don't report mass or energy after magnet operation has begun It appears that, of real magnets, the best cryocooled magnet reported here is 0.335 g/J, while the best superconducting magnet is 0.205 g/J. These numbers can be compared with those of ITER and TPX, tabulated several years ago, during the TPX project, in Table I-2:

Table I-2

Mass Efficiencies of ITER and TPX

Coil System	Stored Energy	Mass	**Mass/Energy**
	(GJ)	(tonnes)	**(g/J)**
ITER CDA			
TF	40.7	6,960 +1500, OOP structure	**0.209**
PF	18.7		
ITER EDA			
TF	108	11,100 (with BC) +5000, OOP structure	**0.148**
PF	25.3	3069	**0.121**
TF+PF	133.3	19,000	**0.143**
TPX			
TF	1.05	138.6 (structure) 51.1 (windings)	**0.181**
PF	0.113	39.0 (windings) 9.0 (structure)	**0.425**
TF+PF	1.163	237.1	**0.204**

Here it appears that most of the coils should be in the range of 0.121-0.21 g/J. The analytical resources applied to ITER were very formidable, but since none of the coils were built, the estimates could still be optimistic.

A possible integrated coil project, discussed at the end of this memorandum, might be to build a coil system with a specific mass of 0.1-02 g/J (or 0.05-0.1 g/J for aluminum magnets), since it appears that this hasn't been done yet.

Reported costs are probably even more difficult to interpret than reported mass efficiencies, because of differences in methods of accounting. Some reported values of cost and specific cost are shown in Table I-3.a-d.

Table I-3.a Specific Cost of the CS Model Coil

Subsystem	Parameter	Cost	Specific Cost
Inner Module			
Strand	6.5 tonnes	$7.8 M	$1200/kg
Jacket	2.5 km (25 tonnes?) 12.2 kg/m CS1 8.65 kg/m CS2	$2.5 M	$1000/m $100/kg
Coil (fab, tooling, development)	39 tonnes	$17 M	$436/kg (44 cents/g)
Subtotal	39 tonnes	$26.3 M	$674/kg (67 cents/g)
Outer Module			
Strand	7.41 tonnes?	$6.9 M	$930/kg
Jacket	2.85 km 29 tonnes?	$2.8 M?	$1000/m
Coil	50 tonnes?		
Subtotal	50 tonnes?	$26 M?	$520/kg?
Precompression Structure	70 tonnes	$0.8 M	$11.4/kg (1.1 cents/g)
Buffer Zone	18.2 tonnes		
CS Model Coil			
	600 MJ	$60 M?	$0.1/J?
	177.2 tonnes	$60 M?	0.295 g/J $338/kg ($0.34/g)

A 1995 interpretation of magnet costs by the PCAST Study Group[1] used the following scaling rules in its derivation of unit cost scalings. A later study added the cost of the TPX coils at the time of the project cancellation:

---

[1]PCAST Study Group, "Technical and Cost Assessment of the PCAST Machine - Final Report," Vol II, Ch 4.0 Cost, 91-951208-MIT/DBMontgomery-01

Table I-3.b PCAST Study Group Magnet Cost Scaling

Magnet Component	(Units)	Value
Manufacturing	($/kg)	56
Copper conductor	($/kg)	12
Magnet Systems		
Copper	($/kg)	68
Superconducting	($/kg)	82
BPX TF Coils	($/kg)	65
TFTR TF Coils	(FY89 $/kg)	103
TFTR TF Cases	(FY89 $/kg)	77
DIII TF Coils	(FY89 $/kg)	98
PF Coil Manufacturing	($/kg)	41
PF Coil System	($/kg)	105
BPX PF Coils	($/kg)	59
TFTR PF Coils	(FY89 $/kg)	180
DIII PF Coils	(FY89 $/kg)	84
Post-PCAST Cancelled Projects		
TPX TF Coils	($/kg)	139
TPX PF Coils	($/kg)	232
TPX CS Coil	($/kg)	332
TPX TF Coils	($/J)	0.11
GEM Solenoid	($/kg)	32
GEM Solenoid	($/J)	0.032

We have not been able to recover the primary sources of the cost data base on which this intepretation was based.

Since the cost of superconducting magnets is frequently confused by other issues, it should also be relevant to try to compare the numbers in the PCAST study with those of commercial magnets. The only large commercial use of superconducting magnets is that of Magnetic Resonance Imaging dipoles, with or without high field homogeneity requirements. According to unreferenceable sources, the cost of a commercial MRI magnet with a typical specification of 2 T on axis, 3-4 T Bmax at the magnet, a 1 m bore, and a length of 2 m would have a stored energy of 4.0 MJ. The fabrication cost for a persistent mode magnet would be ~ $200 k and the sale cost would be $350 k. If the field homogeneity requirements were removed, the cost to the vendor would go down to $180 k. Using an "optimized" sale cost of $300 k for a low field homogeneity system, the specific cost would be $75/kJ or 7.5 cents/J.

A related field of considerable interest is the recent attempt to commercialized large Superconducting Energy Management Systems (SEMS), because the $/J is the single most critical parameter for this application. We would suspect that a well-designed SEMS system would always have a better specific cost than the best fusion system, because it is far less topologically constrained and has no nuclear radiation. Two large SMES systems have been designed and costed in the past two years by BWXT. The first was an 1800 MJ system to be installed in Anchorage, Alaska. This project was cancelled, because of unfavorable cost/benefit analyses. The comparison was with gas turbines. If the magnet system had been compared to fusion magnets, it would have been a world-record breaker. As of April 1997, the entire 1800 MJ x 31.5 MVA SMES system (magnet, refrigerator, and power supply) was costed at $18 M ($0.01/J, $0.57/W). Some of the funding from the Anchorage project was transferred to a SMES project in Kentucky, costed at 30 M$ and 16 M$ for the magnet in a 100 MJ system. The specific cost is then $0.16/J. The cost is driven up significantly by the fact that it must be interfaced with an existing 25 kV bus. A summary of the specific cost of large commercial systems is shown in Table I-3.c

Table I-3.c Specific Costs of Large Commercial Superconducting Magnets

System	Status	Stored Energy	Cold Mass	Cost	$/kg	$/J
		(MJ)	(tonne)	(M$)	($/kg)	($/J)
MRI	Commercial	4.0		0.35		0.075
SMES/Anchorage	Demo/ Cancelled	1800	690	18	26	0.01 ($0.57/W)
SMES/KY	Demo/ Final Design	100		30 (system) 16 (magnet)		0.3 0.16

Finally, the costs of the surveyed magnets should be compared to the costs estimated for ITER magnets. The ITER magnet costs are arbitrarily recosted by multiplying by 10/6, solely on the overall multiplier between system costing in 1989 dollars ($6 B) and estimates that the actual cost would be $10 B.

Table I-3.d Specific Costs of the ITER Magnets

ITER System	Stored Energy	Cost	$/J (1989)	$/J (1999)
	(GJ)	(M$)	($/J)	($/J)
TF	97.5	1244	0.0128	0.0213
CS		263		
PF	25 (PF+CS)	222	0.0194	0.0323

These numbers are taken from the calibration column of my spreadsheet. I wasn't able to find the official numbers for ITER (but my spreadsheet adds up to $6 B.) We should probably find the official numbers before going further. However, I note the obvious. ITER planned on building large magnet systems for 1-2 cents/J, which can be reinterpreted as 2-3 cents/J in inflated dollars. ITER Model Coils apparently cost 10 cents/J. The estimated cost of the TPX TF system, (a 1.1 GJ magnet system with Nb_3Sn at only 8.5 T) by the end of Preliminary Design was also about 10 cents/J. Since no design improvements could be made between the Model Coils and ITER, the implication is that economies of scale alone would improve the specific cost by a factor of 3-10.

If the ITER costs were indeed aggressive, then the purpose of a successful development program that cuts the cost of magnets in half or in a third would be to validate the ITER costing, not improve upon it.

Because of the need to relate integrated magnet programs to subsystem programs, quantitative discussion of magnet system goals is postponed until the end of this memorandum.

A. Superconductor

A.1 Introduction

Significant progress has been made in superconductors in the past 20 years, much of it funded or in support of the magnetic fusion program. The critical current densities of NbTi and Nb_3Sn have improved at rates approximating 7 %/year. Recent developments in Nb3Sn have produced a new strand, being used both the fusion and high energy physics program, with about 60 % better current density than the ITER HP-I strand and 180 % better engineering current density. A new variant of NbTi, called the Artificial Pinning Center conductor, has been developed, with the promise of providing better performance than NbTi at fields below 5 T at half the price. A new A15 material, Nb_3Al, has shown the possibility of slightly better performance than Nb_3Sn with a strain-sensitivity that may be sufficiently reduced to permit react-and-wind fabrication at high fields. Finally, high-temperature superconductors have begun to be commercialized. They are now the conductor of choice for leads below 15 kA and may also be the best superconductor for small, low-field magnets or smaller, high-field inserts.

A.2 State-of-the-Art

State-of-the-art performance of existing superconductors has tended to be expressed at three operating points with historic significance, but which do not necessarily represent the most relevant range of applications for magnetic fusion. These figures are expressed in Table A-I:

Table A-I: Achieved Values of Jc and Jeff, Present Superconductors

Conductor	B(T)	T(K)	J_c (A/mm^2)	Q_h (mJ/cc +/- 3 T)
NbTi	5	4.2	2700	
Nb$_3$Sn (HP-I)	12	4.2	700	600
Nb$_3$Sn (HP-II)	12	4.2	550	200
High Tc	0	77	700	
			J_{eff} (A/mm^2)	
NbTi	5	4.2	1,200	
Nb$_3$Sn (HP-I)	12	4.2	300	600
Nb$_3$Sn (HP-II)	12	4.2	275	200
High Tc	0	77	210	

Two near-term fusion projects, LDX and KSTAR are attempting to extend the performance of Nb$_3$Sn from that already achieved for ITER. These near-term goals are shown in Table II:

Table A-II: Near-Term Strand-Development Goals

Conductor	B(T)	T(K)	J_c (A/mm^2)	Q_h (mJ/cc +/- 3 T)
HP-III (KSTAR)	12	4.2	850	200
LDX	12	4.2	1,125	600
			J_{eff} (A/mm^2)	
HP-III (KSTAR)	5	4.2	340	
LDX	12	4.2	700	600

A single prototype billet and heat has demonstrated the Jc, Jeff, and Qh performance mandated for both the LDX and the HP-III strand. 1,000 kg of HP-III strand and 100 kg of LDX strand are on order.

A.3 Goals

Based on conversations with vendors, we believe that the following goals can be met simultaneously within the next five years:

Table A-III: Five-Year Strand goals

Conductor	B(T)	T(K)	J_c (A/mm^2)	Q_h (mJ/cc +/- 3 T)
Nb$_3$Sn	12	4.2	1,500	600
NbTi/APC	5	4.2	3,600	
High Tc	0	77	140	
			J_{eff} (A/mm^2)	
Nb$_3$Sn	12	4.2	1,100	600
NbTi/APC	5	4.2	1,800	
High Tc	0	77	250	

Adding some cost goals to the performance goals below, the improvements in strand technology to be achieved are summarized in Table IV:

Table A-IV: Improvements in Strand Technology, Next Five Years

Conductor	Jc (A/mm^2)	Improvement	J_{eff}(A/mm^2)	Improvement	$/kg, now	$/kg, 5 years	Improvement	Improvement $/kA-m Best
NbTi/APC	3,600	33 %	1,800	50	100	50	2:1	2.7:1
Nb$_3$Sn	1,500	2.1:1	1,100	3.6:1	800	500	1.6:1	5.8:1
High Tc	140	2:1	63	3:1	2,000	1,000	2:1	6:1

No individual purchase need be greater than a 50 kg billet. Therefore, it would be difficult to really get an accurate assessment of improvements in cost during this period. Improvements in performance will be easier to evaluate, since a 50 kg billet can provide adequate strand length for even the largest coil between joints. Thus, the performance of prototype billets will always be relevant to production, since there is always the option of using smaller billets, if scale-up is difficult.

Assessment of improvements in cost would be made by using prototype billet costs as a reality check and, hopefully, by the use of improved strand in production-scale purchases, during this period, such as KSTAR.

The improvement of Jeff in superconducting strands is the single most important goal of the next five years for the following reasons: 1) Nb_3Sn strand costs have been a significant fraction of the total magnet costs for both fusion and HEP magnets, 2) strand fabrication has usually been on the machine critical path, 3) purchasing and testing prototype billets is relatively inexpensive and almost always leads directly to conductor improvement, and 4) the combined technique of using Superconductor-Laced Copper Conductor (SLCC) cables, described below, is a nearly certain way of achieving another factor of two reduction in strand weight and cost. Here is one scenario for the consequences of success. The improvement of 2.1:1 in Jc would reduce the weight of Nb_3Sn in ITER from 800 tonnes to 380 tonnes, combined with success in developing SLCC, the weight would be reduced to 220 tonnes. If design efforts in ITER-RC abroad ever get as far as the Advanced Tokamak Burning Plasma Experiment (ATBX) and reduce the size of the coils by a factor of two, the weight would be reduced to 110 tonnes. At one extreme, it was feared that Nb_3Sn strand in ITER might stubbornly remain at $1,000/kg, requiring a Nb_3Sn strand purchase of $800 M. If performance improvements can be combined with the specific cost improvement to $500/kg postulated by ITER, the cost of Nb_3Sn strand for an ITER-RC would be only $55 M. With a focused strand development program, we regard this as doable.

A.4 Plan

The improvement of Jc in a strand is relatively straightforward. At least two prototype billets should be purchased each year, and their critical current, critical temperature, and hysteresis loss should be measured. Despite their somewhat arbitrary nature, 5 T/4.2 K, 12 T/4.2 K, 0 T/77 K should probably be maintained as the reference fields and temperatures used for performance specification of low-field, high-field, and high temperature strand performance, during this period.

The improvement of Jeff is more complicated and can be subdivided into four parts. The first, already discussed, is simply to improve Jc with its associated improvement of Jeff, all other parameters being equal. The second is to decrease the copper/noncopper ratio of the strands. The LDX/D20 preprototype strand demonstrated a copper fraction of only 0.3, while the LDX production strand will have a copper fraction of 0.37. The third is to develop finer strands for a price that is competitive with thicker strands. S. Pourrahimi, working with Supercon, has demonstrated bronze-method strands with a diameter less than 0.1 mm and no stabilizer that meet HP-I specifications. Thus, they would not only have an effective current density that is 2.5 times higher than an HP-I strand with a copper/noncopper ratio of 1.5:1, but the cable might be able to operate at up to twice the overall stablizer current density, as discussed below, because it would have four times the wetted perimeter of a cable based on 0.8 mm strand. Finally, the effect on ramp-rate limitations of high Jeff cables has to be quantified. Ramp-rate limits will undoubtedly be more restrictive when stabilizing copper is moved from the composite strand to adjacent strands. Part of this degradation can be restored by the use of finer strands. The purpose of an R&D and theory program is to identify the design regimes in which the effect on conductor cost is first-order, while any negative effect on ramp-rate limitations is only second order. In order to do this, the most important requirement is to continue the series of ramp-rate limitation tests that were conducted on subcables for the DPC and TPX programs. These tests were terminated with the cancellation of TPX and never revived, because the pulsed magnets used to conduct the tests were rendered nonoperational by the closing of the Francis Bitter National Magnet Laboratory. They have not been duplicated by the National High Field Magnet Laboratory. A new superconducting pulsed solenoid should be built as the standard reference tool for testing ramp-rate limitations. This same magnet can also be used for testing quench detectors, all other pulsed field and cryogenic instrumentation, electrical isolators, and feedthroughs.

The plan for improving Jeff includes the following elements:

1) Build a 10 T x 2.5 T/s x 25 cm warm bore pulsed magnet
2) Purchase and test at least one high Jeff prototype billet/year, with not only high Jc, but also low copper fraction. If the strand performs well, a 27 strand subcable should be fabricated and its ramp-rate limitations measured, including the size and number of precursor/recovery "blips."
3) Purchase and test at least one high Jeff, low diameter strand, every two years. If the strand performs well, a 5 kA, 135 strand subcable should be fabricated and its ramp-rate limtiations measured.

B. Stabilizer
B.1 Introduction

A stabilizer matrix is required in parallel with superconducting material for several reasons, including the protection of the magnet, if it should quench; the stability (recovery) of the conductor against disturbances, and the ability to draw or extrude the superconducting wire to its final size. In most, perhaps all, of the magnets contemplated for the fusion program, the size of a cable or conductor is determined more by the current density limits on the matrix than by the superconductor. Methods that can be used to increase the current density in the stabilizer matrix include the use of internal heater wires, finer strands, faster quench detection, and improvements in conductor fabrication techniques.

B.2 State-of-the-Art

The state-of-the-art can perhaps be best expressed through the single parameter of the stabilizer current density at the beginning of quench (A/mm^2). This can be misleading. For example, the reason that the current density is less than half that of TPX or KSTAR is that there is 100 times as much stored energy in the coil system. If the current density were increased to > 200 A/mm^2, the terminal voltages would either increase to 40 kV or a different type of quench method, such as internal heaters, would have to be developed. This is, in fact, what we recommend, since the approach of this program is that every component's performance must be improved across-the-board. State-of-the-art performance in stabilizer current density is shown in Table B-I.

Table B-I State-of-the-Art Performance in Stabilizer Current Density

Magnet	I_{cond}	A_{cu}	J_{cu}	$t@J^2t=2.9\times10^5$ $(A/mm^2)^2$-s
	(kA)	(mm^2)	(A/ mm^2)	(s)
Tore Supra	1.4	9.9	141	14.4
T-15		80		
Nominal	3.8		48.75	120.3
Extended	5.6		70.0	58.4
US-DPC		58.1		
20 kA (1st quench)	20		344.5	2.41
32.kA (highest Iramp)	32		551	0.942
ITER				
TF HF	46	387	119	20.2
TF MF	46	403.7	114	22.0
TF LF	46	418.2	110	23.6
TPX				
TF	33		200	7.15
CS			219	5.96
PF Outer			160	11.2
HEP Dipoles				
Low Jcu			800	
High Jcu			1400	
High Tc Superconductors	0.030	A_{ag}=0.33	90	

B.3 Goals

The goals of a five-year program to improve stabilizer current density should be separated into three categories: 1) CICC-low temperature superconductors, 2) Dipole/quadrupole (Rutherford cable)-low temperature superconductors, and 3) High-temperature superconductors. Based on analysis, we propose the following goals:

Table B.3 Stabilizer current density goals

Conductor Type	Units	Goal
CICC	(A/mm^2)	350
Quadrupole (Rutherford Cable)	(A/mm^2)	1800
High-temperature superconductor	(A/mm^2)	180

The goals for CICC and Rutherford cable imply the development and use of internal dump by electric heaters. The goal for high-temperature superconductor implies the use of passive self-protection without quench.

B.4 Plan

B.4.i. CICC

The current density of an externally dumped magnet can only be increased to the first order by increasing the dump voltage or decreasing the dump energy by subdividing. Since there are obvious fundamental limitations to either approach, the primary strategy for improving CICC current density will be to adopt a variant on the HEP method of using heater blankets and cowind heater wires along with the cable. These heater wires should also be designed to be used as high-sensitivity quench detectors, as discussed below in Section I. In the ATBX design, we used simple hand calculations to demonstrate that the peak-average ratio of local energy deposition could be held to 10:1, using heaters with 1/100th the power rating requirements of external dump circuits. Therefore, the triple win of this concept is to 1) reduce the cost of interrupter/dump circuits, 2) increase the current density in the copper and 3) provide a "free" quench detection system at the same time.

The first step would be to develop the numerical tools for analyzing quenches whose propagation is enhanced by internal heaters. These tools would then be used to confirm the method's workability in ITER and ITER-RC, then to design an inexpensive demonstration experiment. Based on the experience of QUELL, a well-instrumented quench detection and propagation experiment can give very definitive confirmation of design code accuracy.

B.4.ii Quadrupole (Rutherford Cable)

The current method of installing heater blankets on the inside and outside radius of a well-contained dipole or quadrupole is probably close to the theoretical limits of magnet protectability. Nevertheless, we think that a prototype of a heavy ion fusion driver (HIFD) quadrupole should be built to push the limits, because the HIFD quadrupoles are higher current density and lower field than conventional dipoles, and thus smaller. An increase of the copper current density to 1,800 A/mm^2 should be achievable, just because of the decreased thermal diffusion time. The HIFD program for IRE proposes to build a prototype quadrupole array each year for four years. The demonstration of high copper current density should be made in an early prototype array.

B.4.iii High-temperature superconductors

Doubling the current density in the stabilizer of a high-temperature superconductor should be simple from the standpoint of manufacturing and stability, because they are inherently very stable and the increase in stabilizer current-density doesn't require any additional manufacturing improvements, in superconductor fill-factor, since we had already postulated the improvements in Jc and Jeff. However, the conflict between protection and the improvement of current density is difficult to solve. High-temperature superconductors have the quintuple disadvantage that 1) they have a lower J^2t integral between operating temperature and acceptable hot spot temperature by about a factor of 2 at 77 K, 2) at present the matrix material must be silver, whose J^2t is not as good as copper's , 3) they can never depend on passive protection through rapid propagation of quench, since quench propagation is very slow, 4) the slow quench propagation also makes propagation voltages low and hard to detect, and 5) they are hard to protect with heaters, because much more energy is needed to raise the high heat capacity metals to quench at high temperatures.

Operating high-temperature superconductors at low temperature solves some of these problems and is probably the design of choice in the near-future. However, a more exciting method of enhancing performance is to take advantage of the high heat capacity and low n-value of the high-temperature superconductors to make them intrinsically self-protecting. Unlike passively-protected low temperature magnets, which depend on the speed of quench diffusion through a magnet, a passively-protected high temperature magnet would depend on the high n-values to develop a resistive zone that could discharge the magnet safely without there ever being a local thermal instability (i.e. quench) in the magnet. This phenomenon has been observed in High-Temperature magnet designers. The fusion plan would be to develop the theory and design tools necessary to calculate the regimes in which passive protection was possible. Having developed numerical tools, a demonstration magnet would be designed with a supplementary dump circuit that could straddle both regimes and demonstrate the limits.

C. Structure
C.1 Introduction

Structural materials are required in order to contain the Lorentz loads of the magnetic pressure vessel, to contain pressurized helium in a CICC, especially during quench, and to contain gravitational forces (severe during an earthquake and particularly severe in Levitated Diples, during a loss-of-control

collision). Structural materials must also avoid excessive rigidity in the wrong locations, during thermal cooldown and quench heating. They must be compatible with coil winding, and, where applicable, with winding separation for insulation and with conductor heat treatment.

C.2 State-of-the-Art

The usual measures of structural goodness are the yield strength (MPa), ultimate strength (MPa), and the toughness K_{IC} (MPa-m$^{1/2}$). Frequently these parameters are more important in welds than in structural base material. The yield strength, ultimate tensile strength, and static allowables of several commonly used structural materials are shown in Table C.2-I

Table C.2-I Static Allowables of Structural Materials

Material	Base/Weld	T	YS	SUT	2/3 YS	1/2 SUT	σallow	Ratio
		(K)	(MPa)	(MPa)	(MPa)	(MPa)	(MPa)	
304 LN Full Cold Worked	Base	4	1558	2015	1038.7	1007.5	1007.5	1.5265
304 LN Full Cold Worked	Base	300	1193	1320	795.3	660	660	
304 LN HT	Base	4	800	1600	533.3	800	533.333	2.667
304 LN HT	Base	300	300	600	200	300	200	
304 LN	Weld	4	569	1703	379.3	851.5	379.333	1.942
304 LN	Weld	300	293	658	195.3	329	195.333	
316 LN	Base	4	815	1360	543.3	680	543.333	2.7177
316 LN	Base	300	300	550	200	275	200	
316 LN	Weld	4	720	1100	480	550	480	2.25
316 LN	Weld	300	320	480	213.3	240	213.333	
Incoloy 908	Base	4	1227	1892	818	946	818	1.1415
Incoloy 908	Base	300	1075	1443	716.7	721.5	716.666	
Incoloy 908	Weld	4	1279	1648	852.7	824	824	1.25
Incoloy 908	Weld	300	1062	1316	708	658	658	
Ti-5Al-2.5Sn	Base	4	1450	1570	966.7	785	785	1.96
Ti-5Al-2.5Sn	Base	300	740	800	493.3	400	400	
Ti-5Al-2.5Sn	Weld	4	1510	1380	1006.7	690	690	1.692
Ti-5Al-2.5Sn	Weld	300	785	815	523.3	407.5	407.5	
Inconel 625	Base	4			0	0	0	0
Inconel 625	Base	300	490	900	326.7	450	326.666	
Inconel 625	Weld	4			0	0	0	0
Inconel 625	Weld	300	450	900	300	450	300	
Inconel 718	Base	4	1300	1600	866.7	800	800	1.333
Inconel 718	Base	300	1000	1200	666.7	600	600	
Inconel 718	Weld	4	900	1300	600	650	600	1.5
Inconel 718	Weld	300	600	900	400	450	400	
Aluminum 6061	Base	4	360	500	240	250	240	1.5487
Aluminum 6061	Base	300	290	310	193.3	155	155	
Aluminum 6061	Weld	4	260	340	173.3	170	170	1.8219
Aluminum 6061	Weld	300	140	210	93.3	105	93.3333	
Aluminum 7039	Base	4	500	650	333.3	325	325	1.518
Aluminum 7039	Base	300	330	430	220	215	215	
Aluminum 7039	Weld	4	260	360	173.3	180	173.333	1.2385
Aluminum 7039	Weld	300	210	350	140	175	140	
1/2 Hard Copper	Base	4	410	490	273.3	245	245	1.361
1/2 Hard Copper	Base	300	330	360	220	180	180	
Soft Copper	Weld	4	70	400	46.7	200	46.6666	1

Soft Copper	Weld	300	70	200	46.7	100	46.6666	

C.3 Goals

Inexpensive, relatively high performance 300 series steels will remain the low-cost structural materials of choice in both the short and medium term. Although very difficult, it may be possible to develop an alloy during a 5 year period with a combination of higher strength and toughness than Incoloy 908 with the same excellent strain compatibility with Nb_3Sn. However, there are still several issues that remain in guaranteeing the use of the best structural materials in all fusion magnets. These include:

C.3.i) Incoloy development
C.3.i.a) Code qualification of Incoloy 908

A property data base has been developed for Incoloy 908 base metal, welds, and transition joints that has proved to be adequate for the ITER CS Model Coil. In order to use Incoloy 908 in ITER or an ITER-RC and to reduce the ultimate cost of Incoloy 908, the work should be completed in creating an adequate data base for ASTM code qualification. During the ITER program Extension of the data base for 908 still requires characterization of toughness, SAGBO, and crack growth as a function of heat treatment, as well as procedures and characteristics of joints to other materials. Incoloy 908 is relatively well characterized for the ITER heat treatment of 650 C for 200 hours. Other heat treatments of particular interest are the shorter and hotter treatments required by Nb_3Al and high-temperature superconductors.

During the ITER period, advanced weld wire materials were developed at the PSFC with very low degradation of properties during prcoessing. The new weld wires were not developed in time for use in the ITER CS Model Coil. However, an adequate data base can be developed for ITER or ITER-RC. The same is true of the characterization of joints and terminations. A key issue is the guaranteed elimination of helium leakage at the joints.

The quantitative goal of complete qualification of Incoloy 908 is to generate broad acceptance of the material and reduce the specific cost by a factor of two from \$40/kg to \$20/kg.

C.3.i.b) SAGBO resistance in Incoloy

Fusion programs, beginning with the US-DPC magnets and concluding with the ITER CS Model Coil have developed the procedures for welding and heat treatment of Incoloy 908 so that embrittlement by Stress-Aggravated Grain Boundary Oxidation (SAGBO) does not occur. However, the risk of accident can be greatly reduced if a variation on the 908 alloy were developed with the same or even better mechanical properties, but more resistance to oxidation. Incoloy 908 can develop SAGBO at high tensile stress with an oxygen content of 0.1 ppm. Our goal is to develop an Incoloy series that is simultaneously stronger and tougher than 908 at cryogenic temperature and that resists SAGBO at any stress up to an oxygen content of at least 10 ppm, or an improvement of at least 100.

C.3.ii) Toughness of 300 series steel after heat-treatment

300-series steels such as 304LN or 316LN are less expensive and better qualified than Incoloy 908 for most applications. However, for the long heat treatments needed for Nb_3Sn, they are actually less well characterized. **The superiority of Incoloy 908 over 316LN is that it was designed to be compatible with Nb_3Sn heat treatments, over a broad range of temperatures and times. This is particularly important for internal tin designs, which tend to require heat treatments of 250-300 hours. For example, the toughness of Incoloy 908, K_{IC} = 235 MPa m$^{1/2}$ at 275 hr at 700 C.** The toughness of 300-series base metal and welds degrades significantly, during long heat treatments. A typical curve is shown in Figure C.3.ii-1:
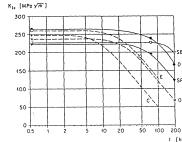
Figure 4. Fracture toughness at 4 K versus heat treating time at 700°C. In addition to the steels C, D and E values of Ogata[a] and new test results of Shimada[b] are included (designated by O and SB and SP, respectively). - - -, interpolated curves.

In order to survive the heat treatment, using 316LN, a low carbon steel, enriched with nitrogen was used. Reed and Walsh have shown that chrome carbide embrittlement can be avoided by reducing the carbon content of 316LN[2]. A similar, low-carbon, high-nitrogen 316LN was used by the National High Field Magnet Laboratory in the 45 T Hybrid Nb_3Sn Outsert coil. This material was designed for only a 90 hour heat treatment, and required a very low carbon content and consequently a high specific cost of $26/kg. The TPX and KSTAR Nb_3Sn 's require 260 hour heat treatments: a regime where it can be seen that there is no data base at all and reason for concern that there will be severe degradation for all known 300 series steels.

The goal of a 300 series steel development program would be to characterize a 300 steel whose strength and toughness would be no worse than that of 304LN with a weld toughness of at least 250 MPa-$m^{1/2}$ after a 700 C heat treatment of 260 hours and a specific cost of no more than $10/kg.

C.3.iii Welds and transitions in Copper Alloy Plates

Several low-cost burning plasma experiment concepts involve the use of high-strength, high-conductivity plate materials. These might use either copper alloys with a good combination of strength and conductivity or sandwiches of a better conducting material, such as copper, and a structural material, such as steel. It has recently been suggested that the best combination of materials for a given mission might be a sandwich of copper alloys and copper. In previous designs of this sort, such as the Burning Plasma Experiment (BPX), the base beryllium copper had an allowable operating stress of ~ 430 MPa. However, the allowable stress in the welds was only ~ 175 MPa. Discussions with vendors indicate that beryllium copper plates can be welded with stress limits up to 90 % of the base metal.

The goal is to develop welding and bonding techniques, along with design analytical techniques that permit a primary membrane stress in the throat of a next-step TF magnet of at least 400 MPa with an averaged J^2t of at least 8 x 10^{16} A^2-s/m^4 (double the allowable for BeCu in BPX).

C.4 Plan

Incoloy 908 welds and brazes to Monel should be characeterized until there is an adequate data base to obtain ASTM code stamp approval for use in pressure vessels.

Work should begin in developing a second-generation Incoloy with high working stress, toughness, and SAGBO resistance than Incoloy 908. The goals should include:
1) Yield stress > 1400 MPa
2) KIC after a 300 hour burn at 700 C > 300 MPa-$m^{1/2}$.
3) No SAGBO at any stress at oxygen concentrations up to 10 ppm.

300 series steels should be characterized with high enough carbon contents to be economical, but with adequate resistance to heat treatments to achieve weld toughnesses of KIC > 250 MPa-m $m^{1/2}$ after a 300 hour burn at 700 C.

C.a Conductor/Structure

C.a.1 State-of-the-Art

---

[2] R.P. Reed R.P. Walsh, and C.N. McCowan, Adv. Cryo.Eng., V.38, 45, 1992

In advanced, high-field normal magnets, it is necessary for the conductor to also be a strong structural material. In general, this means that the conductor should be either a high-strength alloy of copper or a copper/structure lamination, such as copper/steel. Both copper alloys and copper/steel laminates tend to lie upon a "classic" tradeoff curve between strength and conductivity. Two examples of these curves are given in Tables C.a.1 and C.a.2.
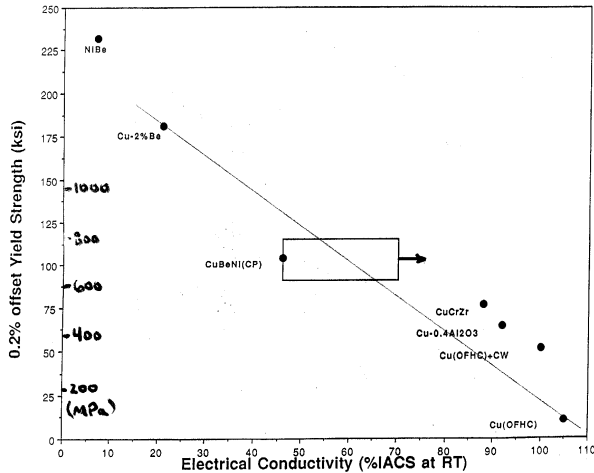

Table C.a.1 Yield Strength (ksi, MPa) vs. %IACS of Candidate Copper Alloys (coutesy I. Zatz, Princeton Plasma Physics Laboratory)
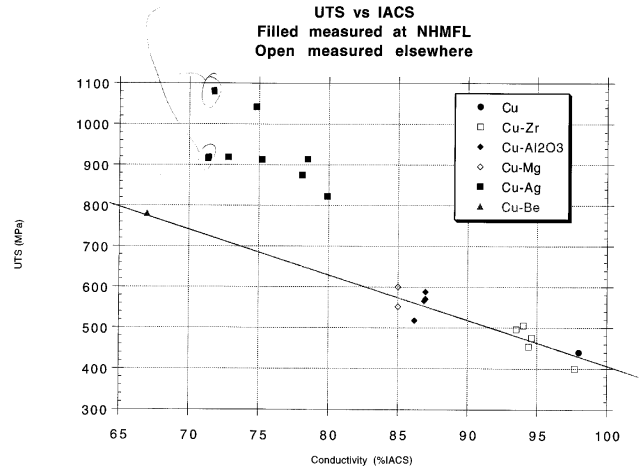
Table C.a.2 Ultimate Strength (MPa) vs. %IACS of Candidate Copper Alloys (courtesy M. Bird, R. Walsh, National High Field Magnet Laboratory)

Most copper alloys and copper/structure laminates follow approximately the following two equations:

$$\mathbf{s}_{YS} = 360 + K_{YS}(100 - \%IACS) \qquad \text{C.a.1}$$
$$K_{YS} = 13.3$$
$$\mathbf{s}_{UTS} = 400 + K_{UTS}(100 - \%IACS) \qquad \text{C.a.2}$$
$$K_{UTS} = 11.4$$

The range of validity of these equations is approximately 70-100% IACS. Measurements of the performance of Cu-20%Ag in Japan and the National High Field Magnet Laboratory indicate that it is possible to develop plates in practical sizes that can raise K_{UTS} from 11.4 to 23 MPa/%IACS and K_{YS} from 13.3 to 17.4 MPa/%IACS[3]. A 16 T solenoid was built with this alloy. Supercon has developed NbCu plates with similar characteristics. The disadvantages of the the more advanced alloys are (1) that they are not available in the range of sizes needed for burning plasma experiments ~ 0.5-5.0 cm x 20-50 cm or lose strength at higher thicknesses, (2) they are very expensive ($100-$300/kg), and (3) they don't have multiple vendors and the silver alloy has no domestic vendor.

C.a.2 Goal

Work with a US vendor to develop a practical copper alloy plate in sizes useful for near-term and proposed burning-plasma experiments with a value of K_{UTS} of at least 23 MPa/%IACS and K_{YS} from 13.3 to 17.4 MPa/%IACS from 70-95%IACS.

C.a.3 Plan

Identify a US vendor willing and capable of developing the required size and capacity plates. If none, identify a foreign vendor. Prepare and test small samples of candidate alloys over range of thicknesses, test the G-function (A^2-

---

[3] Y. Sakai et al, "Development of high-strength, high-conductivity Cu-Ag alloys for high-field pulsed magnet use," Appl. Phys. Lett. 59 (23), 2 Dec 1991, p.2965; S. Miura et al, "Development of large scale CuAg Bigger Plates for the Hybrid Magnet," Proc 15th Magnet Technology Conference, Beijing, China, Oct 20-24, 1997, p.683

s/mm^4) from 30 K to 300 K, as well as resistivity and strength. Manufacture prototype plates in minimum and maximum thickness.

D. Insulation
D.1 Introduction

Electrical insulation is needed to prevent leakage current and arcs due to magnet voltages during charging, discharging, and quench dump. The insulation must be able to withstand voltages that to date have gone as high as 25 kV. They must also act as a key structural element in maintaining winding pack stiffness or allowing local expansion, strain sharing, and load bearing in a conductor in plate design. Where insulators can develop tensile loads, they must have adequate shear strength to prevent tearing. In the front layers of a toroidal field magnets, insulation must also be able to withstand neutron and gamma irradiation. The ability to withstand this radiation is frequently the magnet limit that determines the thickness of the neutron shield.

D.2 State-of-the-Art

Individual components in insulation systems are frequently ranked by their compressive strength (MPa), shear strength (MPa), and dielectric strength (kV/mm). The properties of some candidate insulations are listed in Tables D.2-I-III.

Extensive insulation materials screening was done as part of the U.S. ITER Insulation Program. A report on materials screening results exists in a series of viewgraphs by Schutz of Composite Technology Development[4]. The results of the screening are tabulated below:

Table D.2-I Candidate VPI Resin Systems Screening Tests at 76 K
Short beam shear test for apparent interlaminar shear strength

Resin Type	Resin System	Apparent interlaminar shear strength	Coefficient of Variation
		(MPa)	(%)
Flexibilized DGEBA	CTD-101K	108	4
DGEBA	Shell 826	112	113
DGEBA	ER-321	84	4
DGEBA	VRI-3407	64	10
Polyesterimide	VRI-3308	23	5

Table D.2-II: Candidate Prepreg Resin Systems Screening Tests at 76 K
Short beam shear test for apparent interlaminar shear strength

Resin Type	Resin System	Apparent interlaminar shear strength	Coefficient of Variation
		(MPa)	(%)
DGEBA Epoxy	SP-250	63	1
DGEBA Epoxy	XP-1003	64	1
DGEBA Epoxy	BASF-5216	34	2
DGEBA Epoxy	LTM-12	27	1
TGDM/DGEBA Blend	JDL-552	51	6
TGDM Epoxy	CTD-112P	108	6
Bismaleimide	CTD-200P	37	6
Polyimide	CTD-320P	41	6
Polyimide	AFR-700	110	3

---

[4] J.B. Schutz, "Materials screening for ITER TF coil insulation," Proceedings of ITER Workshop on U.S. Insulation Program and OFE Base Program Review of Low-Temperature Structural Alloys," Oct 12 and 13, Hyannis, MA

Table D.2-III: Candidate VPI Resin Systems Screening Tests at 4 K and 76 K
45° Shear/Compression Strength

Resin Type	Resin System	Shear/Compression Strength	Coefficient of Variation
		(MPa)	(%)
76 K			
Flexibilized DGEBA	CTD-101K	176	2
DGEBA	Shell 826	171	7
TGDM	CTD-110X	137	7
4 K			
Flexibilized DGEBA	CTD-101K	178	3
DGEBA	Shell 826	177	5

Schutz's conclusions were that DGEBA epoxy systems were superior to other VPI resin systems and that TGDM epoxy systems were unsuitable for ITER. Flexibilized DGEBA (CTD-101K) and DGEBA (Shell 836) resin systems were selected for further evaluation in the ITER irradiation program. CTD-101K was ultimately selected. By contrast, Schutz concluded that TGDM and polyimide prepreg systems were superior to DGEBA, DGEBA blend, and BMI resin systems. TGDM (CTD-112P) and polyimide (AFR-700) resin systems were selected for further evaluation.

Schutz also provided a summary table of the dielectric strength of the candidate insulation systems.

Table D.2-IV: Dielectric Strength at 76 K of Candidate Insulation Systems

Material	Specimen Thickness	Breakdown Voltage	Dielectric Strength
	(mm)	(kV)	(kV/mm)
VPI epoxy systems			
CTD-101K/2 plies 6781 glass fabric	0.53	40	76
Shell 826/2 plies 6781 glass fabric	0.52	46	88
VPI epoxy systems with barrier			
CTD-101K/6781 glass fabric/Kapton HA	0.55	>50	> 90
CTD-101K/6781 glass fabric/IM1498-37B Mica	0.57	>46	>82
Prepreg epoxy systems			
CTD-112P/2 plies 6781 glass fabric	0.55	44	80
CTD-105P/2 plies 6781 glass fabric	0.64	34	53
JDL-552/2 plies 6781 glass fabric	0.58	30	51
CTD-1PFS/2 plies 6781 glass fabric	0.59	46	77
Prepreg epoxy systems with barrier			
CTD-112P/1 ply 6781 glass fabric/IMI 498-37B	0.63	49	78
CTD-112P/1 ply 6781 glass fabric/VRI #6293	0.5	42	85
CTD-112P/1 ply 6781 glass fabric/MM #553	0.59	>48	>81
CTD-112P/2 plies 6781 glass fabric/Kapton HA	0.57	>46	>82
Prepreg polyimide systems			
CTD-320/2 plies 6781 glass fabric/IMI 498-37B	0.69	>55	>79
AFR 700/2 plies 6781 glass fabric	0.50	>55	>79
Prepreg polyimide systems with barrier			
AFR 700/2 plies 6781 glass fabric/Kapton HA	0.52	49	94

As with the TPX tests, reported below, all candidate insulation systems look quite good. However, the CTD-101K/6781 glass fabric/Kapton HA VPI epoxy/barrier hybrid system is an obvious first choice, since it also has good shear strength. TPX sample tests indicated that EPON 826 had higher performance than CTD 101-K, the ITER choice. Kapton was the best all-around unreinforced polyimide for high dielectric strength.

The combined mechanical and electrical limits of a potted winding pack with rectangular conduits, which does depend upon shear strength was determined by the TPX electrical insulation development program. The following table is a summary of the 3x3 conductor stack insulation model test designs. The pulsed load applied to each stack was 28 MPa on top of a clamped preload of 14 MPa. This approximately doubled the severity of the actual mechanical load on the TPX insulation. Every one of the insulation systems, with the exception of Model 6[5], had excellent performance and thus 1-5 are all good candidates for any high mechanical and electrical stress magnet design. The insulation topologies studied and the results are shown in Table D.2.V.

Table D.2.V: 3x3 Conductor Insulation Systems Tested for TPX

Model	Insulation System	Insulation Details	Corner Roving	VPI System	Turn-turn withstand (kVdc)
1-CDR Baseline	2D S-glass Double thick	TTI Satin weave wrap 3/4" x 0.1" with G-10 L-L barriers	Glass bundle - epoxy	Shell 826	10
2-Slip plane option	Kapton at the conduit with 2D weave overwrap	Kapton H 0.001" with XMPI adhesive , TTI plain weave wrap 3/4"x0.008"	Glass bundle - epoxy	Shell 826	28-39 (post15000 cycles) 30-38 (15,000 cycles+stress to failure)
3-CDR Baseline with Araldite	2D S-glass	TTI plain weave wrap 3/4" x 0.008" with G-10 L-L barriers	Araldite-filled Epoxy	Shell 826	22, RT 5-12 (15,000 cycles+stress to failure)
4A-Interim baseline with 3D Overwrap	Kapton at conduit; 3D weave overwrap	Kapton H 0.001" w/o adhesive and 3D 1"x .014" wrap	3-D Shape Dry (16)	Shell 826	28-38, RT 31-40 (15,000 cycles) 20-35 (15,000 cycles+stress to failure)
4B-Interim Baseline with 3D Overwrap	Kapton at conduit;2-50 %, 0.025 mm thick Kapton, type HN (no adhesive) wraps 3D weave overwrap	Same as 4A. 1-50 %, 0.356 mm thick (thin) 3D S2 fiberglass tape overwrap	3-D Shape Tackified (16), S2 fiberglass woven preform	Shell 826	26-40, RT 28-40 (15000 cycles) + (stress to failure)
5A-Hybrid Prepreg with 3-D Overwrap	Kapton interleaved with 2D glass prepreg; 3D weave overwrap	CNF Plain weave 1" x 0.007" with CTD112P prepreg & Kapton H 1"x0.007" on top with 3-D 1"x0.014" overwrap	3-D Shape Tackified	CTD 101K (No mold preheat)	
5B-Hybrid Prepreg with 3-D Overwrap	Kapton - interleaved with 2D glass prepreg; 3D weave overwrap	Same as 5A	3-D Shape Tackified (12) Dry (4)	CTD 101K (No mold preheat) 101K	<23, RT 0 (15,000 cycles)
6A-3-D Cigar roll	3D weave S-2 glass overwrap	3-D cloth 3.75" x 0.032" with 0.016" seam tabs	3-D Shape Tackified (8) Dry (8)	Shell 826	
6B-3-D Cigar roll	3D weave S-2 glass overwrap	Same as 6A	3-D Shape Tackified (9) Dry (7)	Shell 826	

---

[5] T. Antaya has argued that Option 6 was fabricated incorrectly and that the tests were irrelevant to the fundamental limits of that insulation option.

The baseline design -- kapton over the conduit, a 3D weave overwrap and a 3D tackified corner fill -- was confirmed as the highest performing option. However, all of the options with the exception of the cigar roll had objectively high performance. The superiority of the TPX interim baseline is that when it fails mechanically, it fails through the VPI part of the insulation, without damaging the kapton wrap, so that large through cracks don't affect electrical integrity. Option 2, the kapton slip-plane with 2D overwrap, also had this "belt-and-suspenders' advantage over the other three design options.

The intrinsic dielectric strength of the best solid organic insulations exceeds 500 kV/mm. However, in service, the electrical field in an organic insulation is unlikely to exceed 2 kV/mm. In ITER, the maximum design electric field in the TF insulation was 5 kV/mm in 4 mm or 1.25 kV/mm. In TPX, it was 500 V/mm. The electric field in KSTAR is not known yet, but since the insulation is the same thickness as TPX' and the terminal voltages are lower, it should be below 500 V/mm.

D.3 Goals

D.3.i Higher specific performance in the insulation

The transmission line practice of allowing 2 kV/mm in an epoxy-glass system and 10 kV/mm in kapton has not yet been adopted by the fusion community. An obvious and inexpensive next-step in reducing the volume and cost of insulation would be halve the thickness of the insulation. This can be done either by halving the number of glass fabric plies from two to 1 or by using plies of half the thickness. For rectangular, potted winding packs, the interturn resistance can be reduced from 1.6 mm to 0.8 mm. This has a second benefit of reducing the bending in the corners of the conduits, because of reduced insulation compliance. It has a third benefit of reducing the cusp area in which it is hardest to avoid resin-rich regions. In an ITER TF-like design with individual ground wraps around each conductor, insulation thickness is also useful as a cushion between the conductor and plate, during a quench, when the conductor expands from overpressure and heating.

The overall goal should be to reduce the insulation thickness by a factor of 2.5 for square conduits in winding packs and by 1.5 for conduits in plates. The goals can be restated as validating design to 1.25 kV/mm, nominal, in winding packs and to 2 kV/mm in conductor in plate.

D.3.ii Compatibility with heat treatment

The process of insulating a winding can be simplified if insulation can be applied during winding, then the winding and its insulation go through the heat treatment together. This is followed by vacuum impregnation. The cost savings in winding and insulation are counterbalanced by any damage to the insulating material or degradation during the winding and heat treatment. Significant testing has been done in Europe on different glasses and ceramics, showing that ceramics and some variants of S-glass show little degradation during heat treatment.

Another difficulty in putting the insulation through the heat treatment is the possibility of contaminating the surface of the conductor conduit with sizing or water vapor. In a famous or infamous experiment at the National High Field Magnet Laboratory, an Incoloy 908 conduit was destroyed by SAGBO, after heat treatment with its insulation. Outgassing of water from the insulation was blamed for the SAGBO, although this was never established. A specific goal would be to demonstrate the compatibility of Incoloy 908 with external insulation, either by 1) proving that water vapor was not the cause of the NHFML failure, 2) eliminating the failure mechanism by shot-peening, 3) developing an Incoloy alloy, as mentioned above with higher resistance to SAGBO, or 4) improving the desizing/baking techniques to maximize glass strength, while minimizing outgassing. The specific goal would be to demonstrate at least two orders of magnitude safety margin in water-outgassing for an insulation and Incoloy system.

The overall goal of the compatibility task would be to equal ITER and TPX performance (i.e. 1.25 kV/mm) in an insulation system that has gone through the heat treatment.

D.3.iii Radiation resistance

The improved electrical performance goals of D.3.i will be demonstrated at radiation dosages up to 10^9 rads in 3x3 stacks of rectangular and at radiation dosages of $> 10^{10}$ rads for a circular conductor in plate. This is a factor of 10 improvement over ITER.

D.4 Plan

D.4.i Higher specific performance in the insulation

The inexpensive TPX insulated conduit stack tests will be repeated with 3x3 stacks of candidate conduit-insulation systems. In TPX, 6 sets of stacks were tested. Here, four stacks should be adequate, including halving the number of glass layers, halving the width of a glass layer, using a potentially improved material, and using a glass with better fill-factor or contraction properties, such as a 3D weave.

D.4.ii Compatibility with heat treatment

A 3x3 stack of rectangular conduit conductors and Incoloy 908 will be heat treated with a preapplied glass fiber insulation, and tested for SAGBO. If there are no signs of SAGBO, the stack will be impregnated. Dielectric strength before and after 20,000 mechanical cycles will be measured. Design to 1.25 kV/mm will be confirmed.

D4.iii Radiation resistance

Improvements in radiation resistance have usually been achieved by identifying and testing improved materials. At this point, it is probably most useful to test and confirm the radiation resistance of insulation systems. In particular, we have been claiming that the ITER TF insulation should be good to high radiation dosages of up to 10^{10} rads and beyond, because the insulation is always in compression with negligible shear. Radiation of a 2x2 cross-section of this insulation should be irradiation to 10^9 rads, 10^{10} rads and 5^{10} rads, if affordable, and the dielectric strength, with and without mechanical load cycles should be measured. The same should be done for 3x3 stacks of rectangular conduit insulation systems, identical to those proposed for the insulation improvement experiments, described above. These should presumably degrade at lower radiations and be less appropriate for the TF plasma-side layers.

Industrial partners have proposed the development of superior insulating materials with simultaneous improvements in insulation strength and radiation resistance. These should be supported through the fusion program or SBIR's. Whenever they become available, 2x2 and 3x3 stacks, identical in topology to those described in the previous paragraph should be fabricated and tested in order to measure the relation between improvements in material properties and insulation system performance.

E. Thermal Isolation

E.1 Introduction

A superconducting magnet operates at cryogenic temperatures from 1.8 K to 80 K. The heat leak from the magnet to the outside world at room temperature must be limited. There are basically three components that isolate the magnet from the outside world: 1) the gravity supports, 2) cold-surface insulation against thermal radiation, and 3) bumpers. The bumpers are used to support off-normal loads, such as earthquakes and plasma disruptions. In the case of Levitated Dipoles, the off-normal loads also include collisions with the vacuum vessel wall.

E.2 State-of-the-Art

E.2.i Gravity supports

Heat leak through gravity supports can be limited by selecting a material with a good strength to thermal conductivity ratio, such as a G-10 column, and by making the support as long as possible. A long column remains as strong in compression as a short column, but the heat leak decreases proportionally with the length. However, many

magnet systems have space limitations and long-length also makes a support more vulnerable to off-normal loads and buckling. Most important, the longer the support column, the larger and more expensive the cryostat. Therefore, the goodness factor for a gravity support should be G=W/(M-L) (W/tonne-m), where M is the cold mass (tonne) and L is the length of the gravity support (m). The material goodness factors for four candidate materials are shown in Table E.2.i-1

Table E.2.i-1 Normalized Strength/Conductivity of Candidate Gravity Support Materials

Material	σ_U RT	k	f_{max}
	Mpa	W/(m-K)	10^4 x N/(W*m)
300 - 80 K			
SS-304	659	12.3	18.26
Inconel X-750	1222	12.5	33.33
G-10CR	420	0.28	511
G-11CR	461	0.28	562
80-5			
SS 304	659	4.5	146
Inconel X-750	1222	5.0	244
G-10CR	420	0.165	2545
G-11CR	461	0.165	2794

The results of Table 1 shows that support of G-11CR has the heat flux almost 17 times less than support of Inconel at 300 - 80 K and 11.5 times less at 80 - 5 K (for the same force and cross section, same pressure and length).

The heat leak through a support structure can be made less than that of the material itself by 1) supporting the structure in tension at a shallow angle, so that the distance along the support is much greater than the distance to the cryostat wall, and 2) creating a convoluted path in compression. Convoluted paths include 1) Nested cylinders, supporting each other alternately at the top and bottom, 2) a meander, and 3) disks with punchouts. The latter are typically used in accelerator magnets where space is at an extreme premium. A typical thermal spacer is shown in Figure E.2.i-1. Recently, a "Pipetron" approach to a Very Large Hadron Collider (VLHC) has been proposed, that could have several hundred kilometers of underground cryostat and requires a very low leak design. The structural spacer proposed for the Pipetron is shown in Figure E.2.i-2.

Figure E.2.i-1 Conventional Dipole Magnet Gravity Support   Figure E.2.i-2 Pipetron Gravity Support

E.2.ii Bumpers

Bumpers can be considered as the series combination of a support column and two radiation surfaces. However, there cannot be any superinsulation between a bumper and the moving structure it is designed to protect. The goodness factor for a bumper is tonnes/W-m, but a collision factor has to be added. For example, if you want to protect a 1 tonne weight against a 10 g collision, the bumper has to support 10 tonnes. However, since the bumper only has to support the high weight for a short time, it is acceptable to have a thermal short during the collision, and apply the goodness factor only to the steady-state thermal leak.

For example, a bumper can have lower heat leak than a gravity support by stacking thin shim stock[6]. Stacking 0.02 mm stainless steel stock achieves an effective thermal conductivity as good as that of G-11 at a pressure of 8-10 MPa. Conductivity continues to decrease a little slower than linearly with pressure, down to 1 MPa. A pinned stack of washers is being used in LDX which requires 10 g bumpers, in order to minimize the heat leak. Somewhat better performance should be achieved by using Inconel X-750 washers. An early version of the LDX bumper design is shown in Figure E.2.ii-1

---

[6] Scott R.B., Mikesell R.P., in "Applied Cryogenic Engineering", ed. by Vance R.W. & Duke W.M., N.Y., J. Wiley & Sons, p. 510, 1962

Hot Wall

MLI

Stack of
Inconel
Plates

Bumper

Thermal Short
(optional)

X Flexible
Rods

Radiation Shield

Springs

Cold Wall

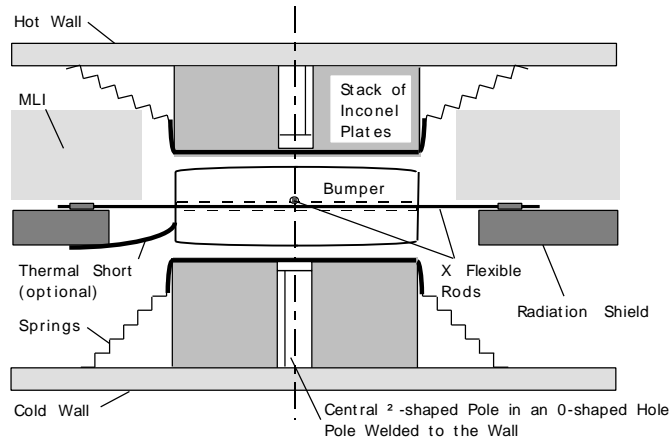Central ²-shaped Pole in an 0-shaped Hole
Pole Welded to the Wall

Figure E.2.ii-1 LDX Bumper Design

E.2.iii Vacuum insulation

Vacuum insulation systems between cold and warm surfaces can be a simple vacuum space alone or contain an insulating material. The most commonly used insulator is a multiple layer of insulators and reflective sheets, called Multilayer Insulation (MLI) or superinsulation. The goodness of a thermal insulation system is its effective conductivity:

$$k_e = \frac{Q''t}{\Delta T}$$

where Q" is the surface heat flux (W/m^2), t is the thickness of the insulation (m), and DT is the temperature difference between the cold and warm surfaces (K). Some representative values of ke are shown in Table E.2.i.

Table E.2.i Effective Thermal Conductivity of Conductive/Radiative Insulations

Material	Temperature Range	Units	ke
Perlite in high vacuum	77-290 K	(mW/m-K)	1.9
Perlite, atmospheric	90-300 K	(mW/m-K)	26-44
Aerogel superinsulation, atmospheric	80-300		8.5-14
Superinsulation in vacuum	80-300	(mW/m-K)	0.05
Superinsulation at 10 mm	80-300	(mW/m-K)	1
Superinsulation at 100 mm	80-300	(mW/m-K)	10

The aerogel superinsulation has about the same apparent density as conventional aluminized mylar at high vacuum. It's advantage is that it is an order of magnitude better than conventional superinsulation at low vacuum and atmospheric pressure.

E.2.iii
E.3 Goals

Develop a gravity support with a specific strength of 10,000 tonnes/W-m or 4 times that of a G-10 column, but with adequate strength to support lateral and off-normal loads.

Develop a bumper support with a specific strength of 25,000 tonnes/W-m or 10 times that of a G-10, with adequate strength to support off-normal bumper loads, including earthquakes, disruptions, and loss-of-levitation collisions.

Develop a thermal radiation barrier with an effective thermal insulation of 10 μW/m-K.

E.4 Plan

Three techniques for reducing steady-state heat leaks or spacing between magnet and cryostat look particularly promising.

1) The use of complex pattern punchings for high strenght - low heat leak gravity supports

2) The use of stacked shim washers for bumpers

and, the, as yet unmentioned, use of:

3) Supermirrors: These are a recently announced technique of applying an extremely reflective, multiple-layer coating to a surface. The effect is much like superinsulation, but without the constraints of mechanical application and the need to maintain "fluffiness." This technique is being investigated for use in the 2 cm gap in LDX. It may be very important in reducing the size of Heavy Ion Fusion quadrupoles, by reducing the gap between the bore and the magnet from 1 cm to 1 or 2 mm.

1) Design studies would be used to optimize the patterns on punched supports. A heavy object (not a superconducting magnet) with conventional MLI would be cooled down and the design analysis verified.

2) A cold press would be applied to a platform supported by pinned washers. The heat leak vs. applied pressure will be measured. Strength vs. compressive and lateral loads will be measured.

3) Several supermirror coatings of different thickness and material combinations will be applied to candidate materials. The material will be cooled down on lightweight platforms and the radiation losses will be measured.

F. Joints
F.1 Introduction

Joints between superconducting cables are necessary at the terminations of every magnet. They may also be needed within a magnet, because of the length limitations of the strands and cable, typically to no more than 1 km or 2 km at the utmost. Joints can also be convenient for layout and assembly of the buswork to avoid pieces that are difficult to transport.

F.2 State-of-the-Art
F.2.1. DC Resistance

The DC resistance of a conventional lap joint can be made arbitrarily small by increasing the area of the joint. The normalized badness factor for DC resistance in a lap joint is $R_{joint} A_{joint}$. A typical state-of-the-art joint for the US-DPC, in which the final stage was spread in a flat blade was 2-3 $\mu\Omega$-mm^2. Joints in which the final stages are left in place generally do worse than that.

F.2.2. Specific Volume

Although there is a fair amount of literature concerning the DC resistance of joints, the volume taken up by a joint and the transitions to a joint, while clearly a cost factor, are almost never reported. Butt joints tend to be far superior to lap joints, even though twice as many joints are frequently needed, as in a hairpin design. The volume of a butt joint should increase roughly with the current. The volume of a lap joint should increases with the 3/2 power of the current, since both the transverse and longitudinal areas of the joint should increase proportionally to the current.
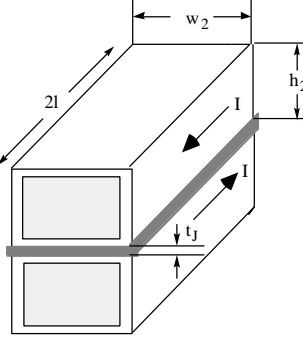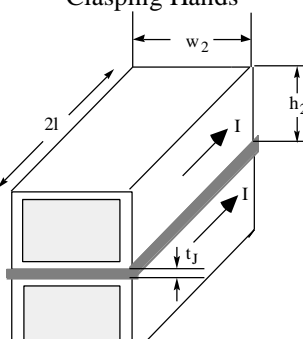
Table F.2.2-I Specific Joint Volumes

Joint	Current	Length	Width	Height	Volume	$V_{Specific}$	$V_{Specific}$
	(kA)	(m)	(m)	(m)	(m^3)	(mm^3/A)	(mm^3/A$^{3/2}$)
ITER US-Prototype	50	0.457	0.089	0.046	1.87 x 10^{-3}	37.4	0.167
ITER US-Prototype (box included)	50	0.72	0.127	0.062	5.67 x 10^{-3}	113.4	0.507

F.2.3 AC Losses

Pulsed losses in a joint are more difficult to characterize and rank for a number of reasons. The first is the intrinsic complexity that they are dependent on the time history and orientation of the field ramp, as shown in Table F.2.3-I.

Summary of Pulsed Joint Losses

	Parallel	Transverse, Broad (Into Plane of Joint)	Transverse, Narrow (In the joint plane)
Flat Lap Joint, Praying Hands	$V = L_{joint} \dfrac{dB}{dt} \sum_{n=1}^{N_{stages}} \dfrac{pr_i^2}{l_p}$ and $P = \dfrac{2V^2}{R} = \dfrac{V^2(h_2 w_2 - h_1 w)}{\rho l}$	$\tau = \dfrac{\mu_0 h_2 w_2}{2(w_2 - w_1)\rho_{jack}}$	$\tau = \dfrac{\mu_0 l\,(t_J + h_2)}{4 w_2\, R_{joint}}$ wherewhere $R_{joint} \cong \dfrac{r t_J}{2 l w_2}$ and $L_{joint} \cong \dfrac{m_0 l(t_J + h_2)}{4}$, $\Delta I = \dfrac{\Delta B w_2}{\mu_0} \dfrac{\tau}{t_{ramp}}\,1/(1 - \tau/t_{ramp})$, $\Delta I\,(\tau >> t_{ramp}) = \dfrac{\Delta B w_2}{\mu_0}$, and $\Delta I(t << t_{ramp}) = \dfrac{\Delta B}{t_{ramp}} \dfrac{w_2 l_2(t_J + h_2)}{2 r t_J}$ [TU91]
Flat Lap Joint, Clasping Hands	$E(V/m) = \dfrac{dB}{dt} \sum_{n=1}^{N_{stages}} \dfrac{pr_i^2}{l_p}$ and $P(W) = \dfrac{E^2(2l)^2 m^2}{3 R_{joint}(\Omega)}$ [MA96] $n \tau_\parallel = \dfrac{\mu_0\, A_{cable,eff}}{12\, l\, R_{join}}$ and $I_{\parallel,\,coupling} = \dfrac{5}{72} \dfrac{A_{cable,eff}\, \dot{B}_\parallel}{R_{joint}}^{2}$ [CI96]	$\tau = \dfrac{\mu_0 h_2 w_2}{2(w_2 - w_1)\rho_{jack}}$	$\tau = \dfrac{\mu_0 l\,(t_J + h_2)}{4 w_2\, R_{joint}}$ where $R_{joint} \cong \dfrac{\rho t_J}{2 l w_2}$ and $L_{joint} \cong \dfrac{\mu_0 l\,(t_J + h_2)}{4}$, , $\Delta I = \dfrac{\Delta B w_2}{\mu_0} \dfrac{\tau}{t_{ramp}}\,1/(1 - \tau/t_{ramp})$, $\Delta I\,(\tau >> t_{ramp}) = \dfrac{\Delta B w_2}{\mu_0}$, and $\Delta I(t << t_{ramp}) = \dfrac{\Delta B}{t_{ramp}} \dfrac{w_2 l_2(t_J + h_2)}{2 r t_J}$ [TU91]
Untwisted cable, lap joint	$V = L_{joint} \dfrac{dB}{dt} \sum_{n=1}^{N_{stages}-1} \dfrac{\pi r_i^2}{l_p}$		

[CI96] D. Ciazynski, "Behaviour of a CSMC hybrid lap joint between a LHH cable and a RHH cable under pulsed field," EURATOM-CEA Note, June 19, 1996

[MA96] N. Martovetsky, "Losses in the parallel field in the joint with the opposite twist in the mating cables," ITER/US/96/EV-MAG/N. Martovetsky/07/05/1

[TU91] B. Turck, "Circulating currents in the superconducting joints of the NET Model Coil and Related Phenomena," NET Memorandum: Note P/EM.91/17

One might try to simplify the design goals as follows. DC resistance is inversely proportional to width x length, while pulsed losses are usually dominated by tranverse field. If the losses are proportional to joint volume x t, then they are proportional to width x length. Therefore, since only pulsed losses threaten stability, wdith should be reduced by not flattening the cable and the length should be shortened until the DC resistance begins rising nonlinearly as the length

becomes less than a twist pitch. However, this approach isn't guaranteed to work for two reasons: 1) The approximation that loss is proportional to Volume x τ is only valid in the fully penetrated regime. However, conventional lap joints in large conductors have time constants of several seconds, while the pulses of greatest interest, such as initiation and disruptions are short.   2) In almost all fusion applications, the integrated refrigeration load from the DC losses is significantly higher than that from the pulsed transient losses, even though the pulsed transient powers are much higher. It should also be noted that butt joints tend to have extremely low pulsed losses, but marginal stability against pulsed losses.

Therefore, this suggests that the best goodness factor for pulsed losses would ignore the loss power per se, and specify the stability against pulsed loads. The ITER joints have been quenching at pulsed loads of ~ 1 T/s at 4 T and 1.5 T/s for parallel field ramps. The range of joint stability results is shown in Figures F.2.3-1 for the ITER US and Japanese TF Prototype Joints. The Japanese joint was a double butt joint with a hairpin jumper between two conductor legs; the US joint is a lap joint. The US Preprototype Joint tests results are not shown, because they were consistently inferior to the Prototype and thus not state-of-the-art. The European ITER joint may be superior to either the US or Japanese joint, but it's pulsed characteristics have not been tested.
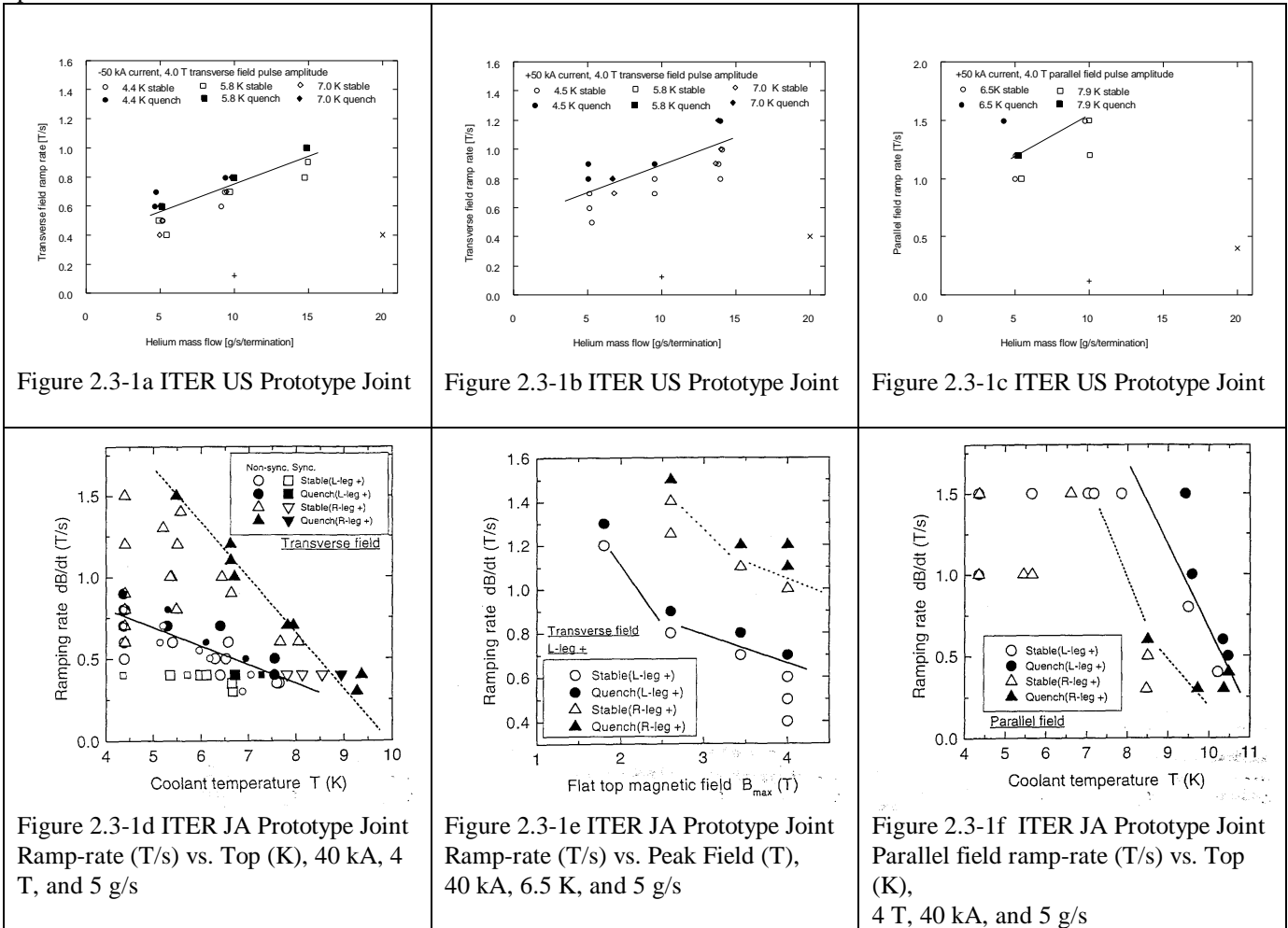

Figure 2.3-1a ITER US Prototype Joint	Figure 2.3-1b ITER US Prototype Joint	Figure 2.3-1c ITER US Prototype Joint
Figure 2.3-1d ITER JA Prototype Joint Ramp-rate (T/s) vs. Top (K), 40 kA, 4 T, and 5 g/s	Figure 2.3-1e ITER JA Prototype Joint Ramp-rate (T/s) vs. Peak Field (T), 40 kA, 6.5 K, and 5 g/s	Figure 2.3-1f ITER JA Prototype Joint Parallel field ramp-rate (T/s) vs. Top (K), 4 T, 40 kA, and 5 g/s

Figure F.2.3-1 Stability limits of the ITER US and Japanese Prototype joints.

Since losses should be proportional to (dB/dt2A joint with an order of magnitude better stability against pulsed losses should be able to ramp at 3 T/s to 4 T.

F.3 Goals

In order to know that a joint is "superior", it should simultaneously improve the goodness factors for volume, DC loss, and AC loss. The goal should be to independently develop joints for NbTi and Nb3Sn with the following properties:

NbTi: A specific volume of less than 1.5 mm^3/A, a specific DC resistance of 0.25 $\mu\Omega$-mm^2, and no quench until a 2.5 T/s ramp up and down to 4 T.

Nb$_3$Sn: A specific volume of less than 15 mm^3/A, a specific DC resistance of 0.5 $\mu\Omega$ - mm^2, and no quench until a 2.5 T/s ramp up and down to 4 T.

The gist of these goals is that a next-generation joint should be superior to the ITER joints in DC loss, volume, and stability by at least an order of magnitude simultaneously in all three categories, and that the NbTi joint should be superior by two orders of magnitude in volume. The specific volumes must include any nonconducting box, but not the specific jumper for a given application.

F.4 Plan

A NbTi "aneurism" joint was developed for the NAVSEA SMES program that achieved the specific volume and specific DC resistance goal for NbTi. AC losses and stability were never tested. The joint is shown in Figure F.4.1. Although not apparent from the picture, the solder joint is also permeable to helium flow. The joint volume is about 1/50th that of a conventional lap joint. The DC resistance was

Figure F.4.1

This joint was only 135 strands, but is expected to scale-up favorably. A similar joint with 486 strands would be fabricated and tested in PTF.

A full-scale Nb$_3$Sn TF coil "Acujuncture" joint was developed for Samsung by M.I.T. as part of the KSTAR program. The joint is shown if Figure F.4.2. The TF conductor in KSTAR has an operating current of 35 kA and 486 HP-III specification (750 A at 12 T x 200 mJ/cc, +/- 3 T) strands. The full-scale sample has been shipped to South Korea to be tested in the new magnet test facility in Taejon. Samsung would send the sample back to the United States for PTF testing, before or after testing in South Korea, depending on the facility completion schedule. The sample may meet all of the goals for a Nb3Sn joint listed above (it meets the specific volume goal). The tests will be analysed and a second generation Acujuncture joint will be designed with specific properties superior to the first. It will then be built and tested in PTF.
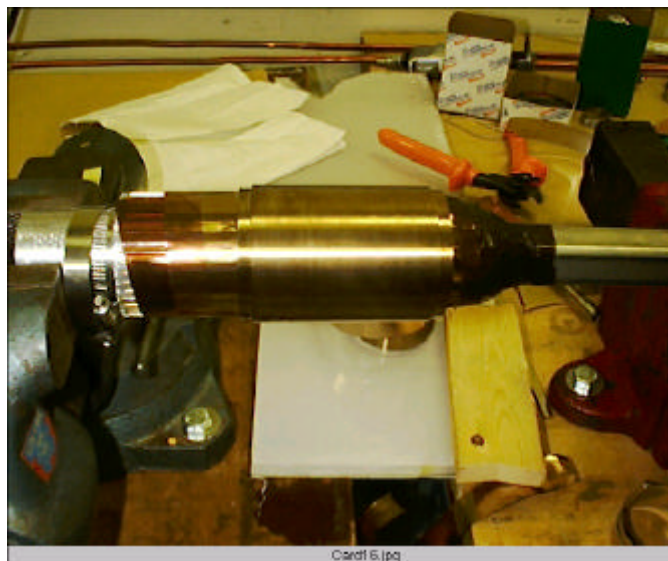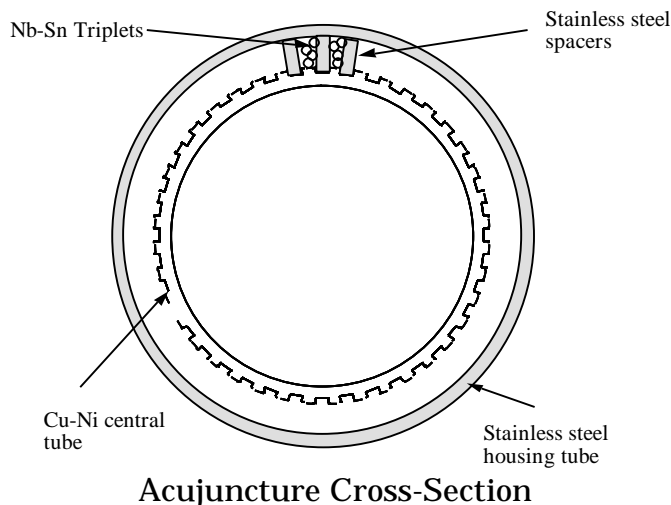
Nb-Sn Triplets   Stainless steel spacers

Cu-Ni central tube

Stainless steel housing tube

Acujuncture Cross-Section

Acujuncture sleeve

Figure F.4.2 The Samsung-MIT KSTAR TF Full-Scale Prototype Joint

G. Leads
G.1 Introduction

The buswork between a superconducting magnet and its power supply requires a transition between the cryogenic environment of the superconducting bus and the room temperature bus to the power supply. Typically, the leads are cooled by helium vapor that traces the vapor-cooled lead vertically from bottom to top. A variation on this method, used only for CICC is to force supercritical helium up through the lead. With the advent of leads using high-temperature superconductors, it is now possible to design leads that cooled by conduction.

G.2 State-of-the-Art

Simple vapor-cooled current leads have an optimized liquid helium requirement of 2.8 (l/hr)/(kA-pair)[7] or 2 W/kA-pair. Commercial high temperature leads achieve 0.4 W/kA-pair. This is actually better than a factor of two improvement, because removing conduction losses doesn't require heating helium up to room temperature, so that that the rate of entropy generation is actually about 6 times better than conventional vapor-cooled leads, rather than 2 times better. The cost of commercial high temperature leads is about $11/kA.

Two lead development programs that are relevant to the US fusion program already exist. The European fusion program intends to develop 60 kA leads, using high-temperature superconductors. The intent would be to use these leads to decrease the operating costs of experimenting with TF prototypes in the TOSKA facility at the Karlsruhe Forschungzentrum (FzK). 10 kA leads have already been designed and tested. FzK does not yet have final approval and funding to build 60 kA leads. The Large Hadron Collider (LHC) has decided to use high-temperature superconductor leads in all of its dipole magnets. These leads will carry 15,650 A for 3520 dipoles/440 cells. The large size of the system may significantly reduce the cost of 15 kA high temperature leads. The efficiency goals are of the program are very high, requiring another two-fold improvement to 0.2 W/kA-pair[8].

---

[7] M.N. Wilson, *Superconducting Magnets*, 265, Clarendon Press, Oxford University Press
[8] Superconductor Week, Dec 31, 1996, Pub by WESTTECH Market information Services

The benefits of using a high-temperature lead are flattened, because of the losses from 77 K to room temperature. According to Hermann[9], the heat load of a vapor-cooled lead at 77 K is 25 W/kA. The heat load value of a conduction cooled lead is 45 W/kA, but can be reduced by the use of a closed-cycle refrigerator.

The optimized value of 1 W/kA-lead for a conventional vapor-cooled lead applies only two a simple copper conductor. Even without the purchase of high-temperature superconducting leads, it is possible to improve the performance of a conventional lead. Some of the design concepts that have been used include:

1) Adding superconducting tape in parallel with the lead to eliminate Joule losses up to the critical temperature.

2) Changing the diameter of the lead at the intermediate heat station

3) Adding fins

4) Having multiple leads in parallel with independent control of liquid level

Historically, any one of these design concepts can achieve an improvement of up to a factor of two in losses.

G.3 Goals

30 kA and 50 kA leads should be developed with performance goals of 0.2 W/kA-pair (6 W/30 kA and 10 W/50 kA) and cost goals of $3/kA. This would be correspond to an improvement of a factor of 10 in losses, 30 in entropy generation, and a factor of 3 in cost vs. present commercial high-temperature leads. As an example, if the system of 45 superconducting magnets in ITER requires approximately 1600 kA (3200 kA-leads), the lead loss would be reduced from 3200 W to 320 W, and the equivalent refrigeration load from about 10 kW to 320 W. There is no high temperature current lead solution at all today, but if we imagine that the coils had all been subdivided into 10 kA segments, the cost of high-Tc leads is reduced from $18 M to $6 M.

G.4 Plan

It is possible, if not probable, that no development is needed in the US fusion program, since the European fusion and HEP programs may develop high-current high temperature leads that achieve our goals. However, since the rewards are relatively high ($12 M in leads, $20 M in refrigeration in a single tokamak), it is prudent to invest at least $100 k-$200 k in prototype lead development. As in the LHC program or TOSKA or in the recent decision by the NHFML 45 T Hybrid program, the most cost-effective method would be to develop/purchase leads that can be dovetailed with another program in order to decrease the operating costs of that program. Two obvious candidates would be to use advanced high Tc leads with the M.I.T. pulsed superconducting coil discussed in the 2 year plan and as leads for the LDX Charging-Coil, the LDX superconducting Levitating-Coil upgrade, or an NCSX superconducting saddle coil option.

H. Quench Detection and Instrumentation

H.1 Introduction

Quench detection is the Achilles heel of a superconducting magnet in an erratic pulsed field environment. The specific weakness of tokamak magnets is the plasma disruption, which is "unscheduled" and varying, making it impossible for its signal to completely zeroed out predictively. Arbitrary reliability can be built into the power supply interrupters through seriesing and redundancy. However, this is much harder to do for quench detectors, that are built into the coils with signal/noise ratioes that intrinsic properties of the sensors. A simplified way of stating the problem is that the magnet

---

[9] P.F. Hermann et al, "Test results of a 1 kA (2 kA)-20 kV HTSC Current Lead Model," Submitted for pulbication in Cryogenics, 17.09.93

voltages are on the order of 10 kV, while the quench signals one would like to detect are on the order of 100 mV, implying a need for 5 orders of magnitude in noise rejection.

H.2 State-of-the-Art

Analysis of scenarios in TPX showed that conventional voltage taps, using bridges across adjacent double pancakes could reduce noise signals to a few volts. Theory and experiment confirmed that cowound sensors, inside the conduit, could reduce the noise further by factors ranging from 400-10,000. The TPX criterion of achieving a signal/noise ratio of 10:1 in time to dump all coils without reaching the allowable hot spot temperature of 150 K was achieved by simulation. Three sets of experiment: the QUELL experiment[10] at EPFL/CRPP, the Noise-Rejection Experiment at LLNL, and the Noise-Injection Experiment at M.I.T[11] all succeeded in achieving very high noise rejection and all agreed with theory to within a factor of two. The QUELL experiment also included a quench detector based on fiber-optic temperature sensing. The unprocessed signal achieved 10:1 signal/noise rejection vs. pulsed loads. Simulation showed that with proper signal processing, the fiber optic sensor would have been superior to the internal voltage sensors.

The QUELL fiber optic detector was based on detecting changes in optical path length, caused by the temperature-dependence of the glass fiber's index of refraction. The fundamental limit on signal/noise in that experiment was distinguishing between path length changes due to temperature and those due to strain in the fiber. Time-dependent strain in the fiber can be reduced by a loose fit of the fiber in its protective can, that decouples it from the Lorentz load strains in the conductor. However, the only way to achieve complete decoupling of strain and temperature is to have two optical signals with different temperature and strain dependencies, then use a multiplier on the phase of one of them, in order to eliminate the strain-dependent signal. This technique was successfully demonstrated on a small NbTi magnet by Steve Smith, using polarity-maintaining fiber and optical signals with orthogonal polarities.

Flow meters may or may not be used as a supplmental method of quench detection. They have the disadvantage of a slow worst-case response, because of limitations in the guaranteed rate of helium flow from the quench zone to the inlet or outlet. They have the advantage that they are external to the coils and can be replaced. The biggest problem with flow meters is that their accuracy is so poor over the high range of operations. Conventional flow meters ,based on the Bernoulli principle, have signals that proportional to rv2. They tend to limited to a dynamic range of 10:1 at best, corresponding to a membrane deflection range of 100:1. The ratio of quench velocity to routine operating velocity can anywhere from 100:1 to 1,000:1. Conventional flowmeters must be protected by bypass valves, which add to cost and clutter and also prevent flow measurements during quench. Conventional flowmeters also suffer from being highly sensitive to changes in temperature and rate of change of field, and frequently to field itself in certain regimes. If they are removed to outside the cryostat, in order to eliminate temperature and field variations, capillary flow tends to damp out the transient flows at the coil inlets that are supposed to be measured. At best, they have accuracies of 2-3 % for steady flow at full deflection. Thus, if they are operated at 1/10 of full range, accuracy can be degraded to +/- 30 %.

The unsolvable problems of conventional flow meters can be removed by the use of optical Fresnel drag meters[12]. These have been shown to work extremely well in water, and have been calibrated at liquid nitrogen temperatures[13]. They have not been calibrated at liquid helium temperatures, and are not expected to be as sensitive. However, they are expected to be accurate to within a few percent at operating flow levels, to become more and more accurate during transients, all the way up to the sound speed of helium, and to be completely insensitive to temperature, field, and rate of field change. They are also beneficial to assembly, because their diameter can be the same as that of the inlet pipes, so they add nothing to

---

[10] J. H. Schultz, ITER No ITER/US/96/EV-MAG/J.H.SCHULTZ/5.31/-1 J. H. Schultz, P.W. Wang, and S. Smith, "Interpretation of Voltage Sensor Data in the QUELL Experiment," May 31, 1996

[11] J. H. Schultz, TPX Memo No: 1314-950709-MIT-JSchultz-01, "Feasibility of the TPX voltage sensor quench detection system," July 9, 1995

[12] R.T. de Carvalho and J. Blake, "Slow-flow measurements and fluid dynamics analysis using the Fresnel drag effect," APPLIED OPTICS, Vol. 33, No. 25, Sept 1994

[13] Joel Schultz, Steve Smith, and V.S. Sudarshanam, TPX Memorandum No. 1314-950817-MIT-JSchultz-01, "Flow meter quench detection system concepts," August 17, 1995

clutter in the helium piping and manifolding, while conventional flow meters and bypass valves frequently limit the size of the cryostat or joint box region.

H.3 Goals

The signal/noise ratioes achieved by ITER and TPX are internal voltage sensors are adequate for all foreseen fusion applications. To achieve universal acceptance of these solutions, the following goals should be achieved:

Demonstration of standoff voltages in voltage sensors of > 500 V, including helium infiltration over a range of partial pressures and over a range of quench/dump temperatures.

Demonstration of leak-tightness of sensor extraction ports over experiment-relevant number of cooldown cycles. Goal should be leak tightness of $< 10^{-6}$ torr after 50,000 cycles.

The intrinsic strain rejection of a fiber-optic thermometer, before filtering and advanced signal-processing, should be reduced by a factor of 10^3, over the range of 4 K-150 K. In other words, a change in the conductor strain of 0.1 % should change the effective differential optical path by no more than 1 ppm. Furthermore, this improvement must be made by the use of external optoelectronics, such as dual color or dual-mode signal injection, and not by the use of expensive, specialized optical fibers.

Attempt to demonstrate feasibility of commercial fiber use with Nb3Sn and high-temperature superconductor. We're not certain that this will work, but the payoff is very large, so a demonstration should be attempted. The idea is as follows. The higher the critical temperature of a superconductor, the more attractive fiberoptic thermometry is for quench detection, because of the rapidly improving temperature sensitivity of the index of refraction. However, the use of commercial fiber with acrylic coatings has been rejected for QUELL, TPX, and KSTAR because it was demonstrated that the coating is destroyed by the high temperature heat treatment. However, since the primary purpose of the acrylic coating is to protect the fiber from embrittlement by water infiltration during handling, it may not be necessary, after heat treatment, by which time the fiber is in a hermetically-sealed protective can. If this is so, the cost of fiber will decrease dramatically from > $10/m to < $1/m, and should continue to decrease as the cost of commercial fiber decreases. This would simultaneously solve the problem of there being a limited number of commercial suppliers of fibers with specialty coatings, such as copper, gold, or graphite.

Develop a flow meter with a dynamic range of 10,000:1 in flow, an improvement of 1,000 over conventional flow meters. Demonstrate 5 % accuracy from 4-150 K and 0 to 10 T/s without signal processing.

H.4 Plan

The strain-rejection experiment performed with a small NbTi solenoid, free to expand, using polarization-maintaining fiber (PM fiber), should be duplicated with commercial fiber, using two mode and two color signal injection. The strain rejection and temperature sensitivities of the two methods should be measured and the better method selected.

A fiber-optic thermometer, using Mach-Zender interferometry and commercial fiber, should be installed in a small CICC, Nb3Sn subcable, and heat-treated. As was done during QUELL development, the fibers should be extracted through one end of the oven, and the thermometer should be used to measure oven temperature during the heat treatment. If the signal disappears during the heat treatment at the point when the coating is evaporated, then the experiment is a failure. If the fibers continue to maintain sealing and temperature signals throughout, the experiment is a highly-probable success, which is then confirmed by cooldown to 4 K and maintaining the temperature signal.

A Fresnel drag flow meter would be fabricated and tested at 77 K and 4.2 K in helium. Sensitivity and ability to reject field, pulsed field and temperature changes would be measured. Multiple pressure and thermal cycles would establish leaktightness.

I. Isolators and Feedthroughs

I.1 Introduction

All magnets are cooled from grounded headers. Since the magnets in a fusion device may have voltages to ground of 10-15 kV, during normal operation or a single ground fault, it is vital to have helium isolators that are guaranteed never to arc over, during a quench, initiation, or disruptions. With the exception of a small effort towards the end of TPX, no work has been done in the United States on this subject. The US is also the only ITER partner that hasn't done any work on helium isolators.   The Germans have pioneered the use of wet-wound, fiberglass-epoxy isolators, because of their ability to take tension as a pressure vessel. However, the use of a wet-wound system guarantees the existence of voids in the isolator and thus the probability of partial discharges during initiation and disruptions that could limit the lifetime of an isolator. Another fundamental problem is that design practice, discussed below, proves little about fundamental limits, because of the large range of design assumptions that have been made. The most aggressive assumption is that one only has to withstand peak voltages at the operating temperature and pressure. The most conservative assumption is that one has to withstand peak voltages at the hotspot temperature. Since voltage withstand is nearly proportional to temperature, this is a difference of up to 40:1. A given experiment, such as the US-DPC, might work perfectly well with a small isolator, because the worst-case conditions never happened; but this could remain a weak spot for an experiment with hundreds of isolators, all of which must work every time for over 10 years.

High-voltage instrumentation feedthroughs must work at high-voltage, in vacuum and in pulsed magnetic field. To the best of our knowledge, only FzK has built instrumentation feedthroughs that operate in conditions that are more severe than those of ITER in the 25 kV POLO experiment. However, the German design is very conservative, using feedthroughs that are so large that they would take up all the available cryostat space in a TPX-size experiment, if they were simply copied there. There are no papers in the literature that discuss the principles of high-voltage feedthrough design and there has been no work on this component in the United States. Late in the TPX program, M.I.T. proposed eliminating high-voltage instrumentation feedthroughs altogether, and replacing them with an all-optical system, discussed below.

I.2 State-of-the-Art
I.2.1 Helium Isolators

The DPC experiment in Japan was operated with 5 kV dump circuits. The POLO experiment generated high pulsed fields with 25 kV induction. ITER was planned for 10 kV operation and TPX for +/- 7.5 kV in the TF circuit. The design practice of POLO and the DPC magnets is tabulated in Table I.2.

Table I.2-I Helium Isolator Design Practice

Helium Isolator	Distance between electrodes	$V_{operating}$	E_{design}
	(mm)	(kV)	(V/m)
US-DPC, Commercial Ceramic	33	3	91
KfK POLO, Stycast/Fiberglass	140	23	164
Ansaldo/NET Stycast/Fiberglass	234	20	85.5
JAERI-DPC G-10 tube	300	5	17

The distance between electrodes of all but the POLO isolator is not accurately known, but is based on interview notes or photographs. The POLO isolator tested is shown on Figure I.2.1. The isolator had been designed and tested at KfK Karlsruhe, and was used for the axial breaks for the POLO Model Coil. The operating voltage of the isolator was 23 kV, and it was tested at 46 kV.
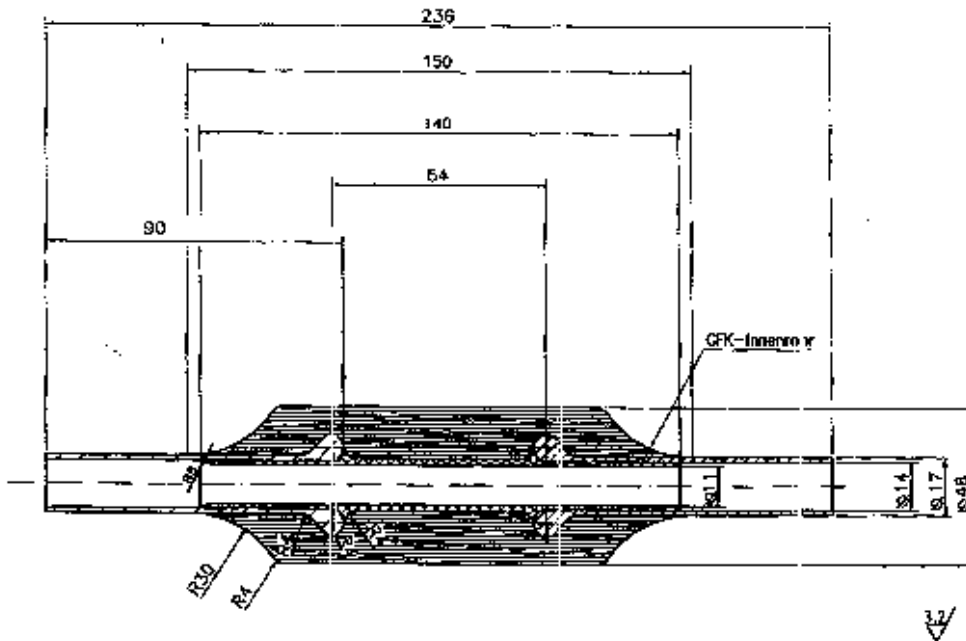
FIGURE I.2.1
KfK Isolator developed for POLO Model Coil

 Notice that at 23 kV/140 mm, they were designed to 164 V/mm (or 328 V/mm, when tested at 46 kV). This is just about double the tracking allowable selected by TPX and KSTAR for organic insulation. The construction of the isolator consists of two stainless steel electrodes, separated by an isolating tube, cast in epoxy and wet wrapped by fiberglass. The "golf club" shape of the electrodes increases the strength of the isolator in tension, and also reduces the peak electrical field. The isolators were built by Lenz, an independent contractor under KfK supervision. The manufacturing process, depends strongly on the skill of the technician, inevitably causes the POLO isolators to have some air bubbles trapped in the insulation[14]. Those bubbles may increase the cooldown shear strength, but decrease electrical strength of the isolator. Partial discharges in those voids may lead to the breakdown of the isolator.

        The differences in sizes and ratings clearly reflect the degree of conservatism in the design. The ceramic isolator and the JAERI G-10 tube with four compression bolts were designed for the same DPC experiment. They differ by 60 % in the claimed voltage capacity, but the JAERI design has about 9 times the length between electrodes, a tube that is intrinsically stronger in tension and that is supplemented by a bolted compression structure that prevents compression. The ceramic isolator was protected by an expansion loop in the helium line to limit the amount of tension in the isolator. This would appear to be an elegant way to allow the use of commercial isolators (all of which are ceramic, we believe), and which probably are more void-free than G-10, wet-wound isolators. However, it is clear that none of the isolators can do anything about the dielectric strength of helium itself. Therefore, it is doubtful that the normalized dielectric strength of one isolator (V/m at fixed T, p) is better than that of any other. Thus, the difference in voltage ratings must be primarily a difference in the conservatism of the designers.

        Let us postulate that the region of most interest is the dielectric breakdown strength of helium at 80 K and pressures ranging from 5-20 atmospheres. The temperature 80 K corresponds to a possible worst case hot spot temperature at the helium isolator that is also an inexpensive temperature for testing, while 5-20 atmospheres covers the probable range of settings for pressure relief valves. The most relevant set of curves[15], showing the intrinsic strength of helium between electrodes in that range is shown in Figure I.2.2.

---

[14] G. Schenk et al, "High Voltage Insulation and Tests of Cryogenic Components for the Superconducting Model Coil POLO", Fusion Technology 1988

[15] B. Fallou et al, "Dielectric breakdown of gaseous helium at very low temperatures," *Cryogenics*, p.142, April 1970
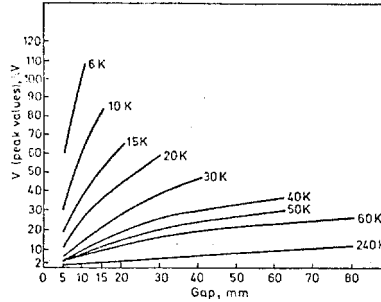
Figure I.2.2 Dielectric strength of helium (kV) vs. Temperature (K) and Gap (mm)

Fallou et al also found that the improvement of dielectric strength with increase in pressure was significantly less than the theoretical linear variation, being only 50 % as the pressure increased from 2 to 10 atmospheres. Unfortunately, although there is an extensive literature on the dielectric strength of helium, the vast majority of the data is wasted for fusion applications, being either for very small gaps, low pressures or liquid helium temperature. This is an area where the data base needs to be improved. If we simply extrapolate from the curves in Figure I.2.2, we might guess that the dielectric strength of a helium isolator should be 300 V/mm (1 atm, 60 K) = 300 V/mm x 1.5 (high p improvement) x 60 K/80 K = 340 V/mm. If we design to 1/2 breakdown - 1 kV, then the POLO isolator should be good for design up to 23 kV at 5-20 atmospheres, which checks. However, since the dielectric strength is clearly saturating with the gap and the pressure, the need to fill in the data base and to be able to interpolate, instead of extrapolating, is obvious.

One possibility for actually increasing the dielectric strength of an isolator was demonstrated by Fast and Hart[16], who showed that filling an evacuated box for power feedthroughs with glass beads increased the Paschen minimum voltage and increased the pressure at the Paschen minimum, as shown in Figure I.2.2. Before they added the beads, they weren't able to hipot at 600 V; when they filled the box with 200-300 μm glass beads, they were. This was followed by testing in an apparatus which permitted breakdown tests as a function of pressure from 1 Pa to 0.13 MPa (10^{-5} to 1 atm) at room temperature, 77 K, and 4.2 K in helium. They found that the minimum breakdown voltage across a 4.8 mm gap was increased by more than a factor of 10 at all three temperatures.

A qualitative explanation for this improvement may be due to electron collisions with glass particles that decrease particle kinetic energy and thus lower the ionizing efficiency. This would tend to increase the Paschen minimum voltage. If the effective gap d between the electrodes is also decreased, because the particles partially fill the volume, and the pd product remains constant at highest ionizing efficiency, then p must increase at the Paschen minimum. A key question is whether the breakdown voltages measured by Fast and Hart really represent an increase of the Paschen minimum from ~ 200 V to ~ 2 kV over all possible conditions, or whether the addition of glass beads has merely converted Paschen breakdown to surface tracking. Clearly, if the Paschen minimum can be raised by an order of magnitude or even more, the failure operating space (the leak/dump design space in which a magnet is operated with high voltage before a leak is detected above the minimum breakdown voltage associated with that leak) can be reduced dramatically.

---

[16] R.W. Fast and H.L. Hart, "Use of glass beads to increase the breakdown voltage in subatmosphere, cold helium gas," Advances in Cryogenic Engineering, V.35, Plenum Press, New York, 1990, pp.809-812
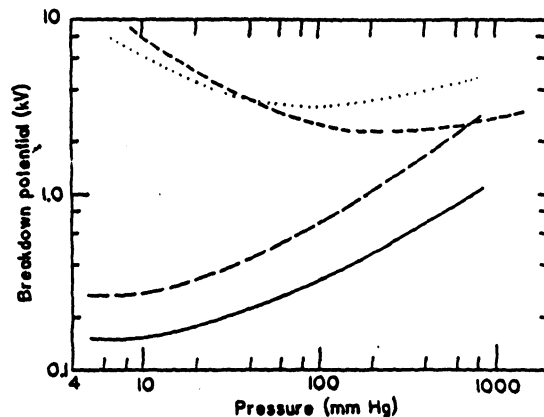
Breakdown voltage as a function of residual GHe pressure:
————, 300 K without beads; — — —, 77 K without beads;
- - - -, 300 K with beads; • • • • •, 77 K with beads.

Figure I.2-2 Paschen curve for helium. (a) Measured in uniform gap and (b) measured in gap with and without glass bead particles

A variation of Fast and Hart's concept could be used in the helium isolators. Here the isolator would be filled with glass beads that are larger and easier to trap with a filter than those used in the evacuated box, perhaps 1 mm glass spheres. If the Paschen minimum can be raised from 160 V to about 2 kV, it will be much easier to design an isolator that will avoid arcing over a broad range of quench and fault conditions. A redundant pair of filter traps would be added at either end of the isolator. If done properly, these can also be designed to help equalize flow in the separate flow channel and to reduce the dynamic range of the inlet and outlet flow from normal operating conditions through quench, in order to alleviate the flow meter protection and calibration problems.

I.2.2 Instrumentation Feedthroughs

Instrumentation Feedthroughs must guide high-voltage sensors through a grounded cryostat, while making a transition between vacuum and air and a gradual transition between pulsed field an no pulsed field. Specific difficulties include 1) allowing a long enough distance along the feedthrough surface to prevent tracking along the surface between hot sensors and ground, 2) preventing high-voltages from developing through space charge on the surface of sensor insulation, and 3) preventing pulsed field from causing low Paschen breakdown voltages in vacuum.

A cable and feedthrough design was developed at FzK that was capable of withstanding the 23 kV of the POLO design, as shown in Figure

I.3 Goals

A helium isolator should be developed with at least three times the dielectric strength at 80 K in helium over the entire range of operating pressures from outlet to inlet pressure relief valve opening. The probable design direction would not be to reduce the helium isolator size by a factor of 10, but to reduce the probability of arcing by six orders of magnitude.

Instrumentation feedthroughs should be developed and tested in vacuum and pulsed magnetic field with no more than 1/10 the specific volume of the POLO feedthroughs.

All optical instrumentation systems feedthroughs should be demonstrated with specific volume no more than 1/100 that of POLO. An optical power supply and voltage-optical converter should be demonstrated for powers up to 100 mW.

I.4 Plan

The use of glass-beads and redundant traps promises to increase the voltage-withstand of a helium isolator by a factor of 3-10. We would fabricate one or more isolators, using beads of different diameter and perhaps with different surface preparation and test their voltage withstand capability over a range of temperatures and pressures. Although we would probably fabricate a new high-voltage, cryogenic test dewar to be coolable to 4 K, the design logic indicates that most or all of the testing should be done at 80 K in helium. In the first place, testing at 80 K is much faster and less expensive. In the second, it is more representative of worst-case hot spot conditions than the dielectric strength at 4 K.

A 10 kV instrumentation cable and feedthrough would be fabricated and tested in the 10 inch, high-voltage cryostat. Breakdown and partial discharge voltages would be measured at different transverse and parallel fields, pulsed field rates, and helium vacuum pressures.

A cryogenic, hot signal converter at 77 K will be demonstrated, including an optical power feedthrough of 100 mW. Along with this, an all optical feedthrough will be demonstrated with a specific volume no more than 1/100th that of POLO.

J. Tolerances and Field-Error
(TBD)
K. Refrigerator
(TBD)

L. Integration

Each of the concept improvements described above has the potential of improving some measure of component cost/performance by a factor of 2:1 or greater. However, it is unclear whether or not the sum of these improvements will also decrease the cost or the size of fusion magnets by a similar or greater amount. The most obvious "dampener" is that no material can be identified that would have double the strength of Incoloy 908; so that structural size requirements will limit the size of a magnet, unless topological improvements are also made. Nevertheless, demonstrations of large improvements in cost or size would increase confidence in magnet systems, as well as improving the overall economics of fusion. Integration can be demonstrated in two ways: 1) The use of advanced magnet systems as subsystems in new physics experiments (e.g. KSTAR, LHD, Wendelstein VII-X, IRE, FIRE, Ignitor, NCSX) or 2) The fabrication of a stand-alone demonstration system (e.g. LCP, DPC, CS Model Coil, TF Model Coil). The advantage of an advanced magnet system in support of a physics experiment is that it doesn't have to justify its existence as a technology demonstration alone, but is necessary for a "far more important" physics mission. The disadvantage is that project decisions always tend towards selecting near-term, less advanced technology, because development is less important than guaranteed performance and the budget and schedule of the physics mission. The advantage of a stand-alone demonstration system is that it can focus on the technology development that is needed by each subsystem, without confusion of goals. The disadvantage is that the overall program is physics-driven, making it hard to justify any expensive technology demonstrators in the short run. Also, the most prominent magnet development programs - LCP, DPC, and the CS Model Coil - all suffered from public perceptions of some degree of failure - perhaps and probably unfairly. In particular, LCP and the CS Model Coil were felt to be overly expensive, while the LCP coil didn't meet its (extraordinarily ambitious) field and ramp-rate goals. We suggest two methods for enhancing the usefulness of the two approaches.

L.A Advanced Magnet Systems in Support of Physics Experiments

Discouragement with superconducting magnet systems has reached a status in the US fusion program in which programmatic mission statements actually specify that next-step plasma burn experiments should use normal magnets. This is greatly at variance with the attitudes of all foreign fusion programs, as well as both domestic and foreign High Energy Physics programs. In our opinion, neither mindset is quite right. Advanced magnets may be either superconducting or normal, and magnet development programs can improve either type of magnet. There is little excuse for not being able to

design magnet systems with any or all of the available technologies and to select the most appropriate technology for each application. That said, it is obvious that superconducting magnets and superconductors have improved more, during the past twenty years, than normal conductors have. It is equally obvious that superconducting magnets will continue to improve more than normal magnets will, because the stoichiometry and properties of superconductors are much more poorly understood than those of normal conductors and there is far more worldwide effort in the improvement of superconductors.

Superconductors should not be selected because of their reactor-relevance, but because of their ability to lower the capital and operating costs of a project. Having recently conducted several design trade studies for various projects, we propose the following crude rule of thumb for the crossover boundaries between superconductors and normal conductors.

1) Superconductors can be smaller and less expensive than normal conductors at fields up to 11 T. For pool-boiling operation at 4.2 K, NbTi is generally preferred over Nb3Sn up to 8-9 T. For CICC operatoin with current-sharing temperatures of 6-7 K, NbTi is generally preferred over Nb3Sn up to 5-5.5 T.
2) High-temperature superconductors are competitive with normal and low-temperature superconductors at fields of 0-1 T. This opinion is counter to the opinion inspired by Jc curves, suggesting that high-temperature superconductors excel at supremely high fields and moderately low temperatures, such as 20 K. The reason for our opinion is that we the excellent high-field critical current densities are counterbalanced by the mechanical weakness of existing high-temperature superconductors. An economic revolution in high-temperature superconductors could occur when they become good enough to be the conductor-of-choice at up to 2 T. At that point, they can displace the copper-and-iron circuits that dominate most of the commercial market.

These rules-of-thumb imply the following for near-term experiments:

Superconductors should be considered for all low-field magnet systems in near-term experiments. These include:

1) The saddle-coils or the discrete-coil options for the National Compact Stellarator Experiment (NCSX). Preliminary sizing indicates that superconductors could halve the size or better of saddle-coils, and that the entire magnet system for either option could be built with existing SSC Rutherford cable.
2) The Heavy Ion Fusion Driver Integrated Resarch Experiment. Preliminary sizing by both M.I.T. and the Lawrence Berkeley Laboratory has indicated that the ambitious goals of 6 T x 6 kA/cm2 quadrupole magnets, using inexpensive automated winding techniques, may be met with the use Artificial Pinning Center strands.
3) The outer PF coils for FIRE or IGNITOR have low enough fields that they could be built in inexpensive, individual cryostats.
4) The 0.8 T Levitating Coil (L-Coil) for the Columbia/MIT LDX experiment is limited by the existing water supplies at the M.I.T. TARA cell facility. The system could be upgraded by the use of a relatively inexpensive high-temperature superconducting coil. The successful completion of such a coil could then lead to more ambitious upgrade coils. The most dramatic would probably be the replacement of the Floating Coil (F-Coil) with a high temperature superconducting coil with the dramatic goal of a full-day float time.

L.B Stand-Alone Advanced Magnet Systems

We would not advocate any stand-alone advanced magnet systems in the next two years, which should be devoted to actually making some of the technical advances described above. After that, however, a stand-alone system might be extremely useful. Here are some ideas for improving the cost-effectiveness of a stand-alone demonstration system.

1) The demonstration system should be relatively small, so that it doesn't consume the magnet development program.   The US-DPC coil is a good example of an inexpensive coil that had several innovations and a large technical impact. We propose that the stored energy of a demonstration magnet be no more than 100 MJ. This is selected as a compromise to be small enough to be inexpensive, but large enough to demonstrate capability and to be useful for power conditioning in a larger experiment.

2) A quantitative demonstration goal should be selected. Specific mass is particularly meaningful. Specific cost is frequently misleading, since it can be affected by historic accident (how many hungry vendors are in the field), first-of-a-

kind, and econonmy-of-scale distortions. It is nonetheless the only reality check there is as to whether concept improvements really are that. The goals of a demonstration magnet should be (1) Specific Mass: 0.1-0.15 g/J cold mass and 0.2-0.3 g/J total system, including cryostat mass (Improvement of 2-3 in specific mass), and (2) $0.01-$0.03/J or an improvement of 3-10 in specific cost over the CS Model Coil. The implication of the cost goal is that a 100 MJ magnet would cost $1-3 M.

3) The coil system should be multipurpose and therefore it must be built at the site of the Next-Step Option, when that site is identified. The importance of site selection to the reduction of US fusion development cost can hardly be overemphasized. The demonstration system should be designed with the following goals in mind: (1) It should have a current and power supply system, so that it will be useful for power conditioning for the next-step option experiment and for future experiments at the same site, such as Prototype and Demo Reactors. (2) It should also be designed to be useful for energy management at the local utility of the Next-Step Option site, so that it can sell power conditioning at a profit during all times that the coil system is not being used for physics experiments. That is, it should assist the Department of Energy in developing large-scale Superconducting Energy Management Systems (SEMS), while greatly improving the competence and confidence of whatever will be our lead fusion laboratory in managing superconducting magnet systems. (3) The system should be toroidal. This has the threefold advantage that it is sufficiently difficult to demonstrate system integration capability, but not so difficult as to significantly drive up the specific cost. Because the toroidal topology has the lowest field leakage, it will also be the easiest to use for SEMS and to qualify against health and integration requirements as specified by limits on interference with pacemakers or nearby instrument rooms. Although perhaps an irrelevant consideration, it also enhances the possibility of additional subsidy by the Department of the Navy, which mandates toroidal systems, so that ship-based SMES systems shouldn't be detectable by enemy submarines.

Summary

The preceding consideration of fusion magnet state-of-the-art and near-term goals is the beginning of a process that should refocus magnet development effort into a more cost-effective program for reducing the cost and improving the performance of magnetic and inertial fusion devices, using magnet systems. At present, we are not prepared to make some of the most important claims that (1) we have identified a program that is compatible with a 5 year schedule, flat or reduced funding, and reduced staffing with other obligations, such as Next-Step Design, Alternative Concept Design, and completion of the Model Coil test program. However, we can make the following claims:

1) Cost-effective development programs have been identified for every one of the major magnet components. In no case, with the possible exception of new superalloy development, do any of the programs cost as much as $1 M.

2) A technical invention or concept is identified for each component with the potential for cost/performance improvements of 2:1 or better.

3) A key component of the magnet development program is the construction of a ten inch bore pulsed magnet to replace the decommissioned magnets of the Francis Bitter National Magnet Laboratory. There are no pulsed magnets, adequate for fusion magnet development, anywhere in the United States and none are planned. This magnet is needed for experiments in ramp-rate limitations, development of the Superconductor-Laced Copper Conductor (SLCC) concept, quench detection experiments, and high-voltage component sensitivity to field and field-ramp experiments.

4) There remains a need to complete the characterization and calibration of many components that were left unfinished at the end of the ITER EDA period. These include qualification of Incoloy 908, heat treatments of 300-series steels, high-voltage ratings in pulsed field of isolators and feedthroughs, flow meter qualification in high transient fields and flows, and quench detector extraction and dielectric strength.

5) The idea is introduced of fabricating one or more multiple-purpose "fusion-SEMS" magnet system in order to demonstrate integration of concept improvements. The overall integration goal is to show improvements of at least 2:1, and hopefully 3:1 in the specific volume and specific cost of an integrated fusion magnet system.